[redacted]

88

Copy
RM L51L28

C-1

NACA

RESEARCH MEMORANDUM

THE EFFECT OF BLADE-SECTION CAMBER ON THE STATIC CHARACTERISTICS OF THREE NACA PROPELLERS

By John H. Wood and John M. Swihart

Langley Aeronautical Laboratory
Langley Field, Va.

[redacted]

CLASSIFIED D[redacted]

This material contains information affecting [redacted] Defense of the United States within the meaning of the espionage laws, Title 18, U.S.C. [redacted] 794, the transmission or revelation of which in any manner to an unauthorized person is [redacted] law.

NATIONAL ADVISORY COMMITTEE
FOR AERONAUTICS

WASHINGTON
April 4, 1952

[redacted]

NATIONAL ADVISORY COMMITTEE FOR AERONAUTICS

RESEARCH MEMORANDUM

THE EFFECT OF BLADE-SECTION CAMBER ON THE STATIC CHARACTERISTICS OF THREE NACA PROPELLERS

By John H. Wood and John M. Swihart

SUMMARY

Static tests have been made on the NACA 10-(0)(066)-03, 10-(3)(066)-03, and 10-(5)(066)-03 two-blade propellers (design lift coefficients of 0, 0.3, and 0.5, respectively). This investigation was conducted on the NACA 6000-horsepower propeller dynamometer at the Langley propeller static test stand. The blades were tested at angles from 0° to 16° measured at the 0.75R station. The maximum tip Mach number was 1.02, but this value was not attained at the 16° blade angle due to blade flutter.

The results of the investigation indicated that the ratio of the static-thrust figure of merit for the cambered propellers to the static-thrust figure of merit for the symmetrical propeller increases with an increase in design lift coefficient over the tip Mach number range; however, the ratio increases at a greater rate than the increase in design lift coefficient at a low tip Mach number and decreases in rate with an increase in design lift coefficient at a tip Mach number of 1.0.

When the blade angle was set at 16°, the propeller with a design lift coefficient of 0.5 fluttered at a higher rotational speed than either the propeller with a design lift coefficient of 0.3 or the propeller with symmetrical blade sections.

INTRODUCTION

Two-dimensional airfoil theory indicates that thin symmetrical sections have higher lift-drag ratios than thin cambered sections at Mach numbers above the shock-attachment Mach number. In an effort to obtain the highest efficiency possible for high-speed propellers, there is a trend, therefore, toward the use of symmetrical blade sections. There is some question, however, whether a propeller having symmetrical blade sections will provide adequate static-thrust characteristics. Some compromise as to the blade-section camber may have to be accepted

in order to provide satisfactory characteristics for both the high-speed and take-off operating conditions.

The effects of camber and solidity on the static characteristics of model propellers, 4 feet in diameter and with a thickness ratio of 0.08, are presented in reference 1, but the propellers used in those tests did not include blades having symmetrical sections. The purpose of the present investigation is to determine the effect of blade-section camber on the static-thrust and torque characteristics of two-blade propellers 10 feet in diameter and with a thickness ratio of 0.066. The blades of these propellers are similar except for blade-section camber, which for each set of blades is constant along the radius. The design lift coefficients for the three blade designs tested are 0, 0.3, and 0.5. The results of the investigation are presented for a blade-angle range from 0° to 16° at rotational speeds up to 2200 rpm.

SYMBOLS

b	blade width, feet
C_P	power coefficient $\left(\frac{P}{\rho n^3 D^5}\right)$
C_T	thrust coefficient $\left(\frac{T}{\rho n^2 D^4}\right)$
C_T/C_P	static-thrust figure of merit
c_{l_d}	design section lift coefficient
D	propeller diameter, feet
h	blade section maximum thickness, feet
M_t	tip Mach number
n	propeller rotational speed, revolutions per second
P	power, foot-pounds per second
r	radius to a blade element, feet
R	propeller tip radius, feet

[redacted]

T	thrust, pounds
x	fraction of tip radius
α_i	induced angle of attack, degrees
α_x	angle of attack of blade element, corrected for induced flow and blade deflection, at radial station x, degrees
β_x	blade angle at station x, degrees
$\Delta\beta$	torsional deflection, degrees
ρ	air density, slugs per cubic foot

APPARATUS

6000-horsepower propeller dynamometer.- The dynamometer consists of two 3000-horsepower units that can be operated independently of one another or as a 6000-horsepower unit. The drive motors are 4600-volt, three-phase, water-cooled induction motors with hollow shafts. Each is rated at 3000 horsepower for 1/2 hour and 4000 horsepower for 5 minutes. The principal arrangements and dimensions of the dynamometer are shown in figure 1. Figure 2 is a photograph of the dynamometer assembly at the Langley propeller static test stand. The three conventional arrangements shown in figure 1 make possible the determination of propeller characteristics in the presence of a hub fairing or air-inlet cowling (fig. 1(a)) and blade characteristics without hub fairing or air-inlet interference as shown in figures 1(b) and 1(c). The propeller blades shown in figure 1(c) are in two stages; each stage can be rotated in either direction independently of the other. For purposes of the present test the forward unit of the dynamometer was removed and only the rear unit was used as shown in figure 3.

Basically the 6000-horsepower propeller dynamometer is similar to the 2000-horsepower dynamometer described in reference 2 inasmuch as the thrust and torque of the propeller are balanced with calibrated pneumatic capsules. The pneumatic capsules consist of three major parts, namely: piston, cylinder, and servo valve. Diaphragms are used to seal the gaps between the pistons and cylinders. The servo valve consists of two parts, one fixed to the cylinder and the other actuated by the movement of the piston. The cylinders are fixed in the direction of the applied force. When the force varies, the piston moves and the servo valve automatically adjusts the air pressure such that the applied force is exactly balanced by the air pressure. In order that a negative

[redacted]

reaction may be measured, the capsule is preloaded by maintaining a given air pressure on the opposite side of the piston. The pressure differential across the piston is measured on scales with the dials graduated in units of pounds of thrust and foot-pounds of torque. The application of a controlled preload on the piston makes the system independent of ambient pressure.

In order that the measurements of thrust and torque reactions be free of friction forces and interactions, a system of flexure plates is used to support the capsule cylinder and the drive motor. The propeller and the capsule piston are mounted rigidly to the motor. The motor support flexure-plate system which is employed at each end of the motor allows the motor, capsule piston, and the propeller a small degree of freedom both axially and rotationally.

The dynamometer is capable of measuring 12,000 foot-pounds of torque at rotational speeds from 300 to 2400 rpm and of measuring propeller thrust from 40,000 pounds to -12,000 pounds.

Static calibration of the thrust and torque measurements gave a probable error of ±3.5 pounds of thrust and ±2.9 foot-pounds of torque. The rotational speed was measured to 1/4 rpm by means of a tachometer which matched the shaft rotational frequency with the known frequency of a tuning fork.

Propeller blades.- The propeller blades were of solid duralumin construction and were designated the NACA 10-(0)(066)-03, 10-(3)(066)-03, and the 10-(5)(066)-03. These propellers are the same ones tested in references 3 to 5. The digits in the propeller designation describe the propeller diameter and the airfoil section at the design radius $\left(\frac{r}{R} = 0.70\right)$ as follows: propeller diameter, 10 feet; section design lift coefficient, 0, 0.3, and 0.5, respectively; section thickness-chord ratio, 0.066; and solidity per blade, 0.03. The blades, which were tested as two-blade propellers, incorporate NACA 16-series airfoil sections and are of a constant chord and camber from the shank to the tip. The blade-form curves for these propellers are shown in figure 4.

TESTS AND REDUCTION OF DATA

The blades were tested at angles from $\beta_{0.75R} = 0^\circ$ to $\beta_{0.75R} = 16^\circ$ in 4° increments. Thrust, torque, and rotational speed were measured in intervals of 100 rpm from 600 to 2200 rpm. A few points were repeated for the purpose of checking values. These blades have not been whirl-tested above 2200 rpm; hence, for reasons of safety this rotational speed was not exceeded.

Considerable saving in time for blade-angle changes was effected by removing the front dynamometer unit and omitting the spinner on the rear unit. Previous tests indicated that a spinner had a negligible effect on the static characteristics of propellers (reference 6).

Wind velocities were measured with a sensitive low-speed hot-wire anemometer. Tests were not conducted if the steady wind velocity was greater than 400 feet per minute or if gust velocities were greater than ±100 feet per minute. No corrections have been made for wind velocity.

The data have been reduced to thrust and power coefficients C_T and C_P. The tip Mach number M_t was based on the rotational tip speed of the propeller.

RESULTS AND DISCUSSION

Typical test results are shown in figure 5. Test points taken after the rotational speed was decreased to the desired value are shown flagged. Faired curves of thrust coefficient and power coefficient against tip Mach number for constant blade angles are presented in figures 6 to 8 for the propellers tested.

Figures 6 to 8 show that there is a gradual increase in C_T and C_P with an increase in tip Mach number for the low blade angles. This increase in the coefficients is in part attributable to Mach number effect and a small part is probably caused by blade twist. At the higher blade angles each of the blades tested showed the adverse effects of compressibility at values of tip Mach number above 0.95. The thrust-coefficient curve either reached a maximum or was decreasing in slope at a value of tip Mach number of 0.95 for all of the propellers. The maximum tip Mach number obtained was 1.02.

Figures 9 to 11 show the variation of static-thrust figure of merit with tip Mach number. The curves show an increase in the ratio of thrust coefficient to power coefficient for the low blade angles until the effects of compressibility decrease the ratio at the higher tip Mach numbers. For the higher blade angles the static-thrust figure of merit is relatively constant with an increase in tip Mach number until it decreases because of critical Mach number effects.

The thrust and power coefficients and the static-thrust figure of merit C_T/C_P have been plotted against blade angle for four tip Mach numbers 0.4, 0.6, 0.8, and 1.0 in figures 12 to 14. These propeller

coefficient curves plotted against blade angle are analogous to lift, drag, and lift-drag-ratio curves plotted against angle of attack.

The effect of camber on the static-thrust figure of merit, C_T/C_P.- The static-thrust figure of merit is plotted against power coefficient in figure 15 for the three test propellers at four values of tip Mach number. For power coefficients greater than 0.02 the curves show an increase in C_T/C_P with an increase in design lift coefficient. The maximum attainable value of the static-thrust figure of merit increases with an increase in design lift coefficient from 0 to 0.3. There is no increase or a slight decrease in the maximum attainable value of C_T/C_P with an increase in design lift coefficient from 0.3 to 0.5 and the power coefficient for the maximum C_T/C_P is higher for the most highly cambered blade.

Figure 16 shows the variation in the ratio of the static-thrust figure of merit for the cambered propellers to the static-thrust figure of merit for the symmetrical propeller with design lift coefficients for tip Mach numbers of 0.4 and 1.0. The ratio increases with an increase in design lift coefficient over the tip Mach number range; however, at the lower tip Mach number the ratio is greater for low values of power coefficient whereas the ratio is relatively independent of power coefficient at a tip Mach number of 1.0. At the low tip Mach number the ratio increases at a greater rate than the increase in design lift coefficient; hence, for tip speeds well below the critical speed, large design lift coefficients will provide the highest static-thrust figure of merit. Compressibility effects, however, reduce the increases in the ratio for more highly cambered blades. The additional benefits of camber decrease from a design lift coefficient of 0.3 to 0.5 and it may be that further increases in camber would show no increase of static-thrust figure of merit for tip Mach numbers greater than 1.0.

Figure 17 shows a comparison of the variation of C_T/C_P with C_P for tip Mach numbers of 0.4 and 1.0. The comparison shows that there is an increase in the static-thrust figure of merit for all the propellers with an increase in tip Mach number at power coefficients greater than 0.02. This increase in C_T/C_P is probably due to the increase in section lift-drag ratio with an increase in Mach number for Mach numbers below the critical (reference 7), since most of the blade sections are operating at subcritical speeds when the rotational tip Mach number is 1.0.

The effect of camber on the stall-flutter speed.- Figure 18 shows the variation of stall-flutter speed with design lift coefficient. At the highest blade angle tested, $\beta_{0.75R} = 16^\circ$, the NACA 10-(5)(066)-03 propeller fluttered at a rotational tip speed of approximately

[redacted]

808 feet per second. This is considerably in excess of the flutter speed of the NACA 10-(0)(066)-03 propeller which was approximately 556 feet per second. It has been found during these tests that the flutter speed can be measured only to within 10 percent, and the data quoted above represent a mean of the two values shown for each propeller. The torsional rigidity of these blades has been previously investigated (reference 8), and it was found in a static bench test that the torsional deflection $\Delta\beta$ for the same applied moment was very nearly equal for both propellers. The first torsional frequencies of these two blades were checked in a bench test and found to be approximately equal. The frequencies were found to be between 151 and 156 cycles per second for the two blades. These results indicate that there is no structural difference in the two propellers to cause different stall-flutter speeds.

If flutter were due to simple stalling or incipient stall of the blade sections (ignoring, for the present, blade twist and assuming equal values of induced angle), the propellers would be expected to flutter at equal values of blade angle and rotational speed because airfoil data (reference 7) indicate that both the NACA 16-0XX and NACA 16-5XX sections stall at approximately the same angle of attack. However, at stall the NACA 16-5XX sections operate with higher lift coefficients than the NACA 16-0XX sections, and therefore the sections of the NACA 10-(5)(066)-03 propeller operate with greater induced angles than do the sections of the NACA 10-(0)(066)-03 propeller. Since the angle of attack of a blade section at zero advance is given by $\alpha_x = \beta_x - \alpha_i + \Delta\beta$, the sections operating with the higher induced angles and the lower torsional deflections will have the lower angles of attack. Reference 8 shows that the NACA 10-(0)(066)-03 propeller had approximately 1.5 times the torsional deflection of the NACA 10-(5)(066)-03 propeller at the same rotational speed, advance ratio, and blade angle. This difference in blade twist was seen as a result of the difference in pitching moment for the sections of the two propellers. Either or both of these factors, the difference in blade twist and the difference in induced angles, are believed to cause the sections of the NACA 10-(5)(066)-03 propeller to operate at lower angles of attack than the sections of the NACA 10-(0)(066)-03 propeller at the same blade angle and rotational speed. If this is true, then the NACA 10-(0)(066)-03 propeller would experience stall flutter at a lower rotational speed than the NACA 10-(5)(066)-03 propeller when operating at the same blade angle. However, further research on the effect of camber on stall-flutter speed will be necessary for an analysis.

CONCLUSIONS

The results of this investigation to determine the effect of camber on the static characteristics of three 10-foot-diameter propellers with

[redacted]

design lift coefficients of 0, 0.3, and 0.5 from blade angles of 0° to 16° and up to a tip Mach number of 1.02 lead to the following conclusions:

1. The use of camber in the propeller design offers advantages in propeller performance and increases the stall-flutter speed at zero advance.

2. The thrust coefficient was adversely affected by compressibility at values of tip Mach number above 0.95 for all the test propellers at the higher blade angles.

3. The maximum attainable value of the static-thrust figure of merit increased when the design lift coefficient was increased from 0 to 0.3. Further increase in design lift coefficient resulted in a slight decrease in the maximum value of the static-thrust figure of merit at the higher tip Mach numbers.

4. The ratio of the static-thrust figure of merit for the cambered propellers to the static-thrust figure of merit for the symmetrical propeller increases with an increase in design lift coefficient over the tip Mach number range investigated; however, the ratio increases at a greater rate than the increase in design lift coefficient at a low tip Mach number and decreases in rate with an increase in design lift coefficient at a tip Mach number of 1.0.

5. At the highest blade-angle setting used, $\beta_{0.75R} = 16°$, the NACA 10-(5)(066)-03 propeller fluttered at a higher rotational tip speed (approx. 808 fps) than either the NACA 10-(3)(066)-03 or 10-(0)(066)-03 propellers. The NACA 10-(0)(066)-03 propeller fluttered at approximately 556 feet per second.

Langley Aeronautical Laboratory
National Advisory Committee for Aeronautics
Langley Field, Va.

[redacted]

REFERENCES

1. Platt, Robert J., Jr.: Static Tests of Four Two-Blade NACA Propellers Differing in Camber and Solidity. NACA RM L8H25a, 1948.

2. Corson, Blake W., Jr., and Maynard, Julian D.: The NACA 2000-Horsepower Propeller Dynamometer and Tests at High Speed of an NACA 10-(3)(08)-03 Two-Blade Propeller. NACA RM L7L29, 1948.

3. Steinberg, Seymour, and Milling, Robert W.: Pressure Distributions on the Blade Sections of the NACA 10-(0)(066)-03 Propeller under Operating Conditions. NACA RM L50C03, 1950.

4. Maynard, Julian D., and Murphy, Maurice P.: Pressure Distributions on the Blade Sections of the NACA 10-(3)(066)-033 Propeller under Operating Conditions. NACA RM L9L12, 1950.

5. Evans, Albert J., and Luchuk, Wallace: Pressure Distributions on the Blade Sections of the NACA 10-(5)(066)-03 Propeller under Operating Conditions. NACA RM L50B21, 1950.

6. Gilman, Jean, Jr.: Static-Thrust and Torque Characteristics of Single- and Dual-Rotating Tractor Propellers. NACA MR, June 28, 1944.

7. Lindsey, W. F., Stevenson, D. B., and Daley, Bernard N.: Aerodynamic Characteristics of 24 NACA 16-Series Airfoils at Mach Numbers between 0.3 and 0.8. NACA TN 1546, 1948.

8. Gray, W. H., and Allis, A. E.: The Torsional Deflections of Several Propellers under Operating Conditions. NACA RM L51A19, 1951.

[redacted]

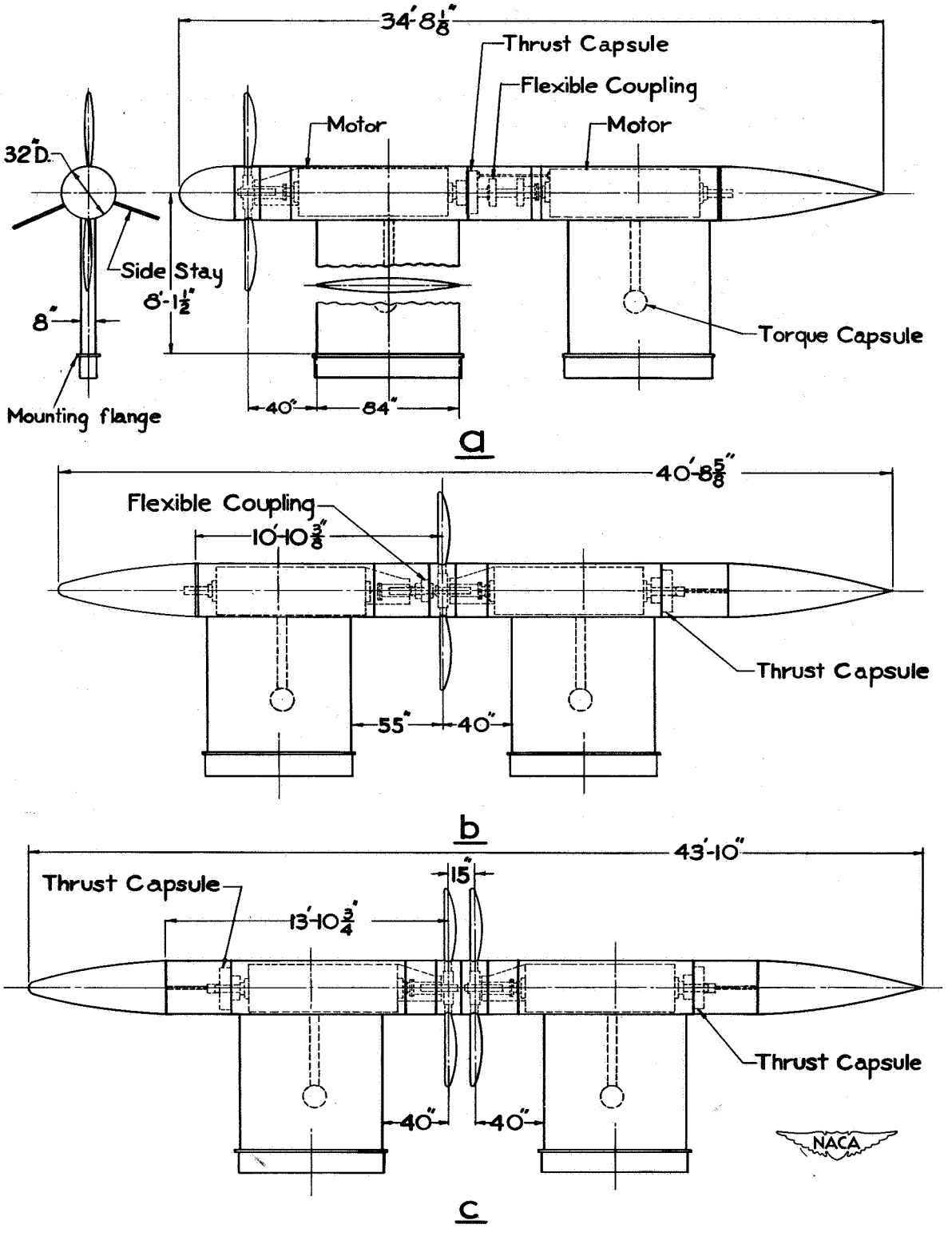

Figure 1.- NACA 6000-horsepower propeller dynamometer.

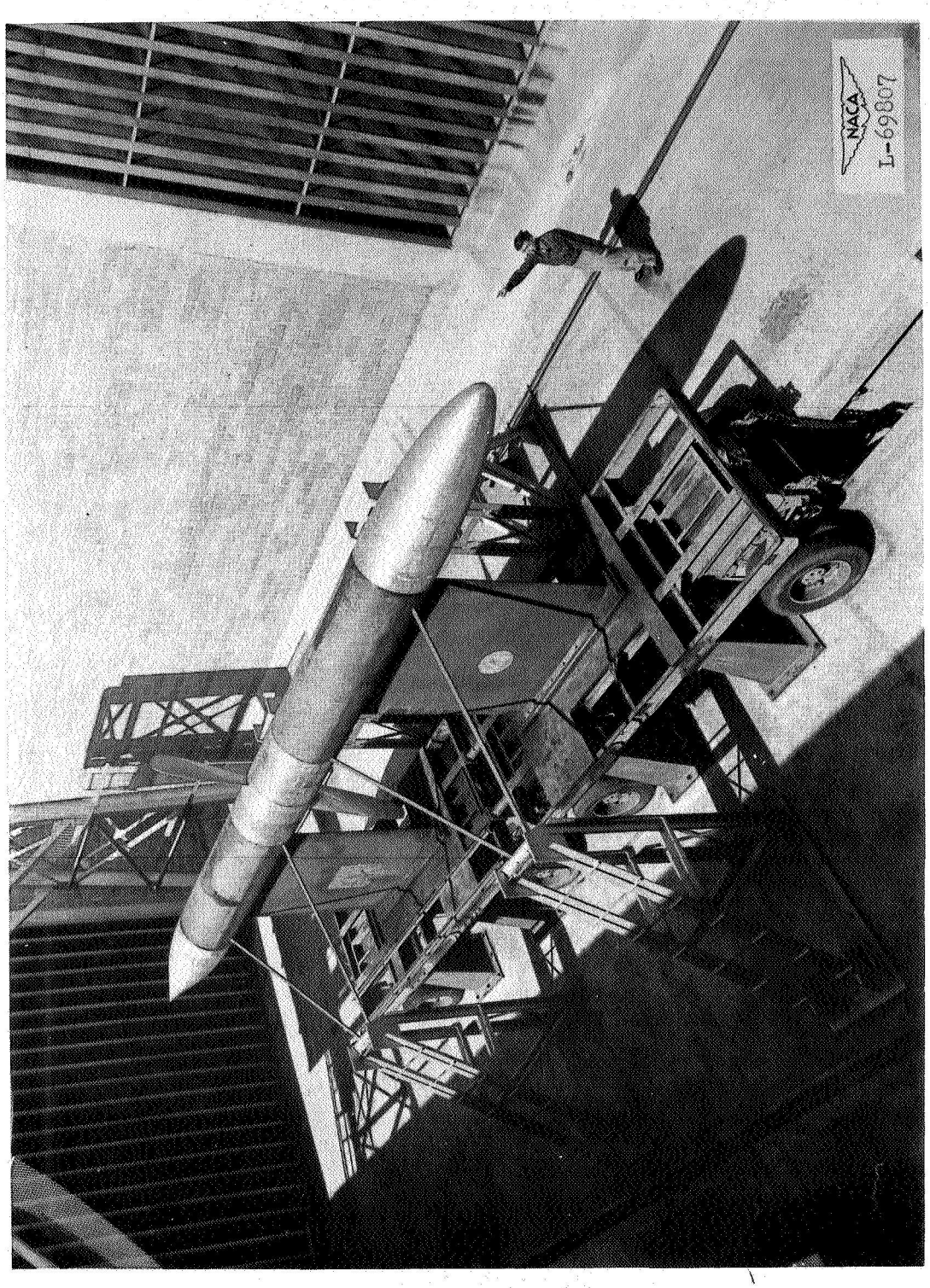

Figure 2.- NACA 6000-horsepower propeller dynamometer.

[redacted]

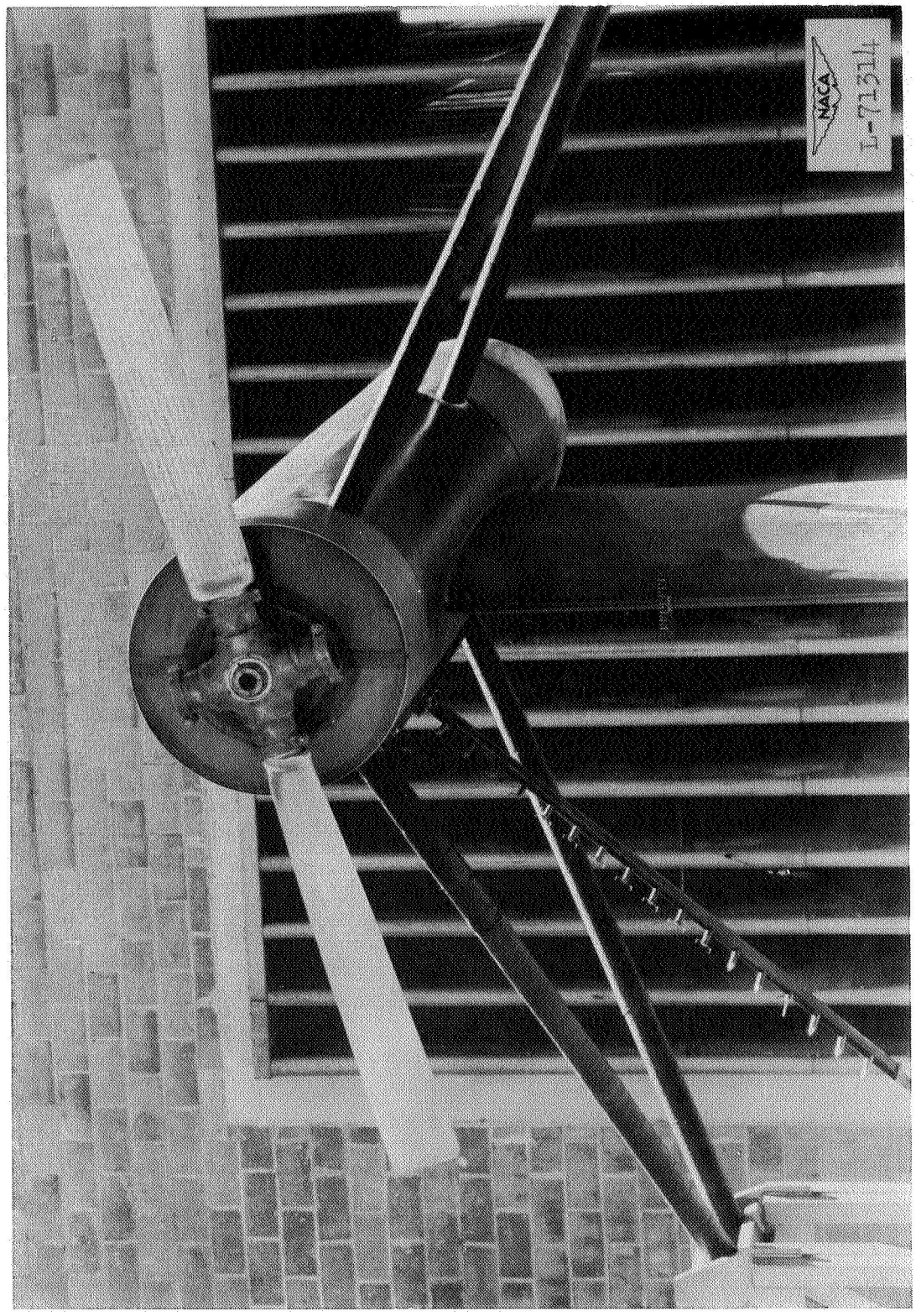

Figure 3.- Rear unit of NACA 6000-horsepower propeller dynamometer.

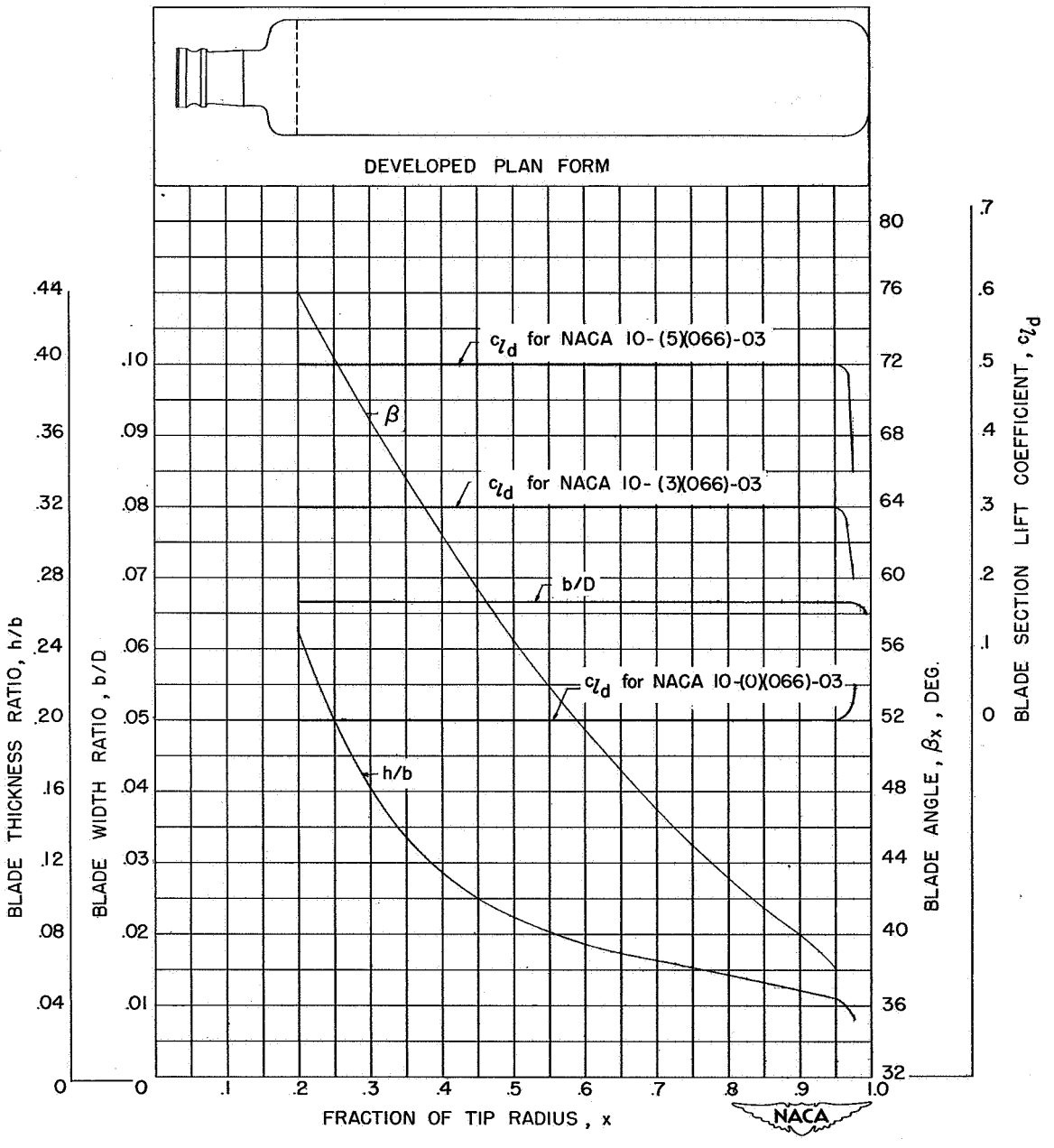

Figure 4.- Blade-form curves for NACA 10-(5)(066)-03, NACA 10-(3)(066)-03, and NACA 10-(0)(066)-03 propellers.

[redacted]

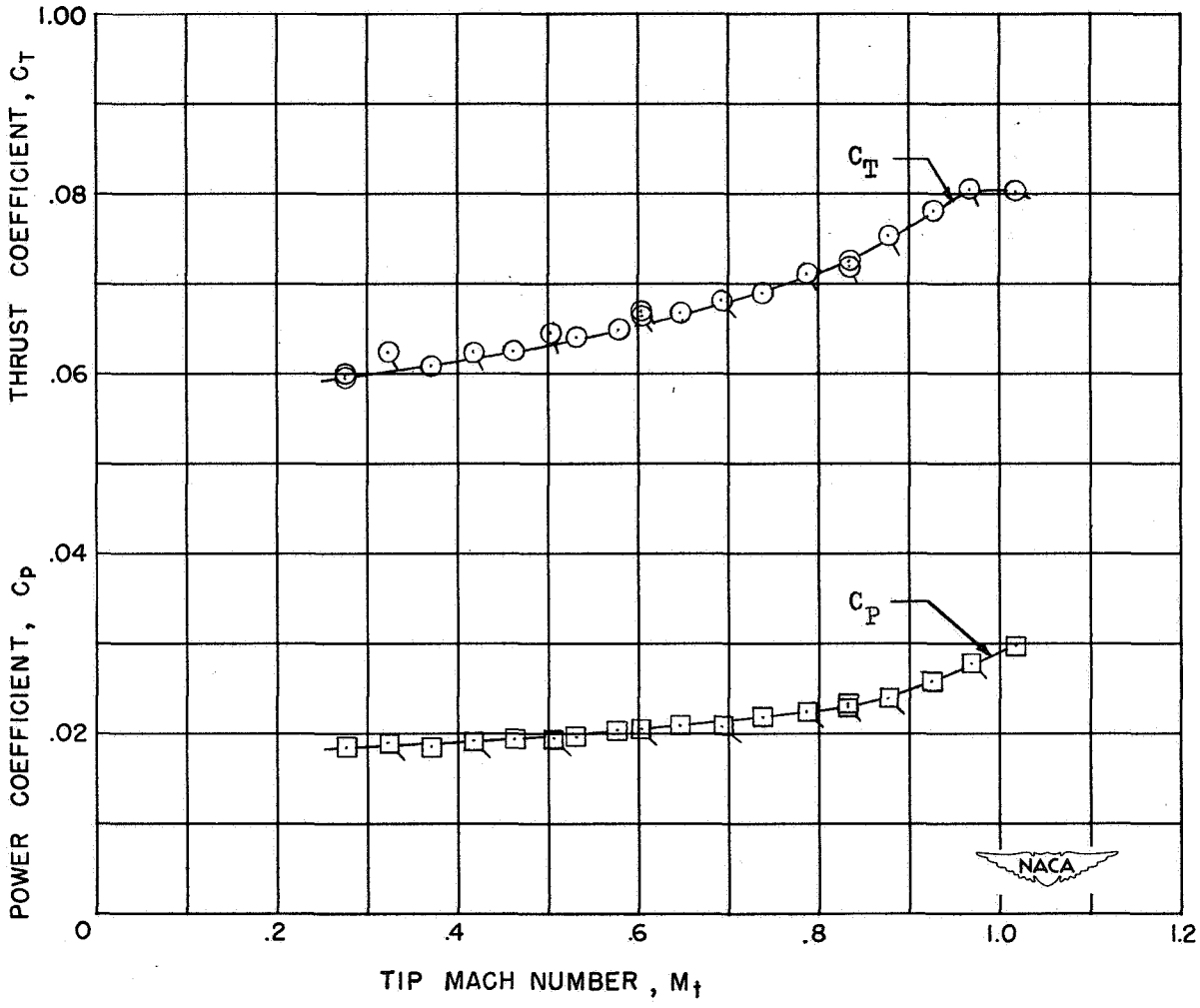

Figure 5.- Typical test results. NACA 10-(5)(066)-03 propeller, two blades; $\beta_{0.75R} = 8^{\circ}$. Flagged symbols indicate data taken with rotational speed decreasing.

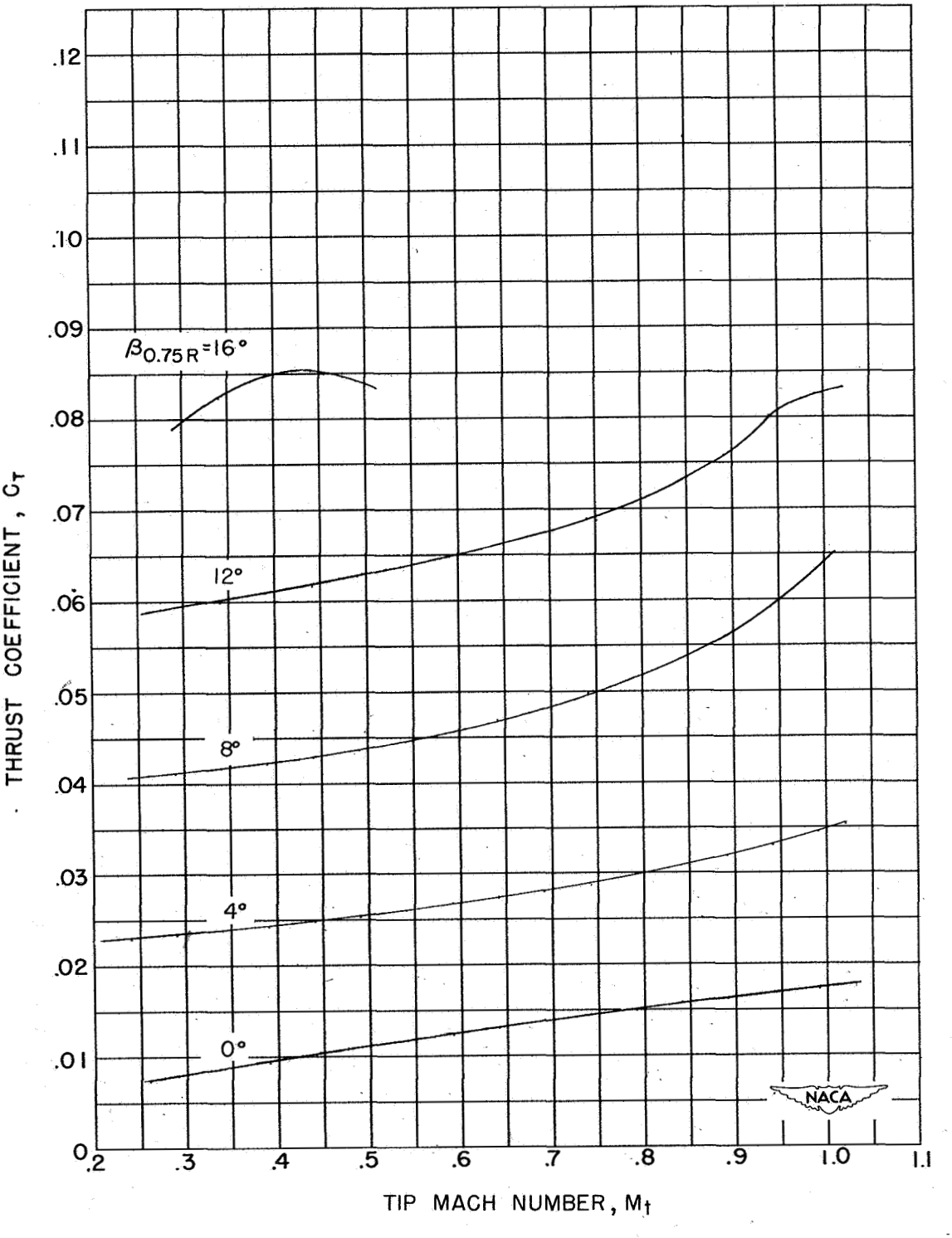

(a) Thrust coefficient C_T.

Figure 6.- Variation of static characteristics with tip Mach number for a two-blade NACA 10-(0)(066)-03 propeller.

[redacted]

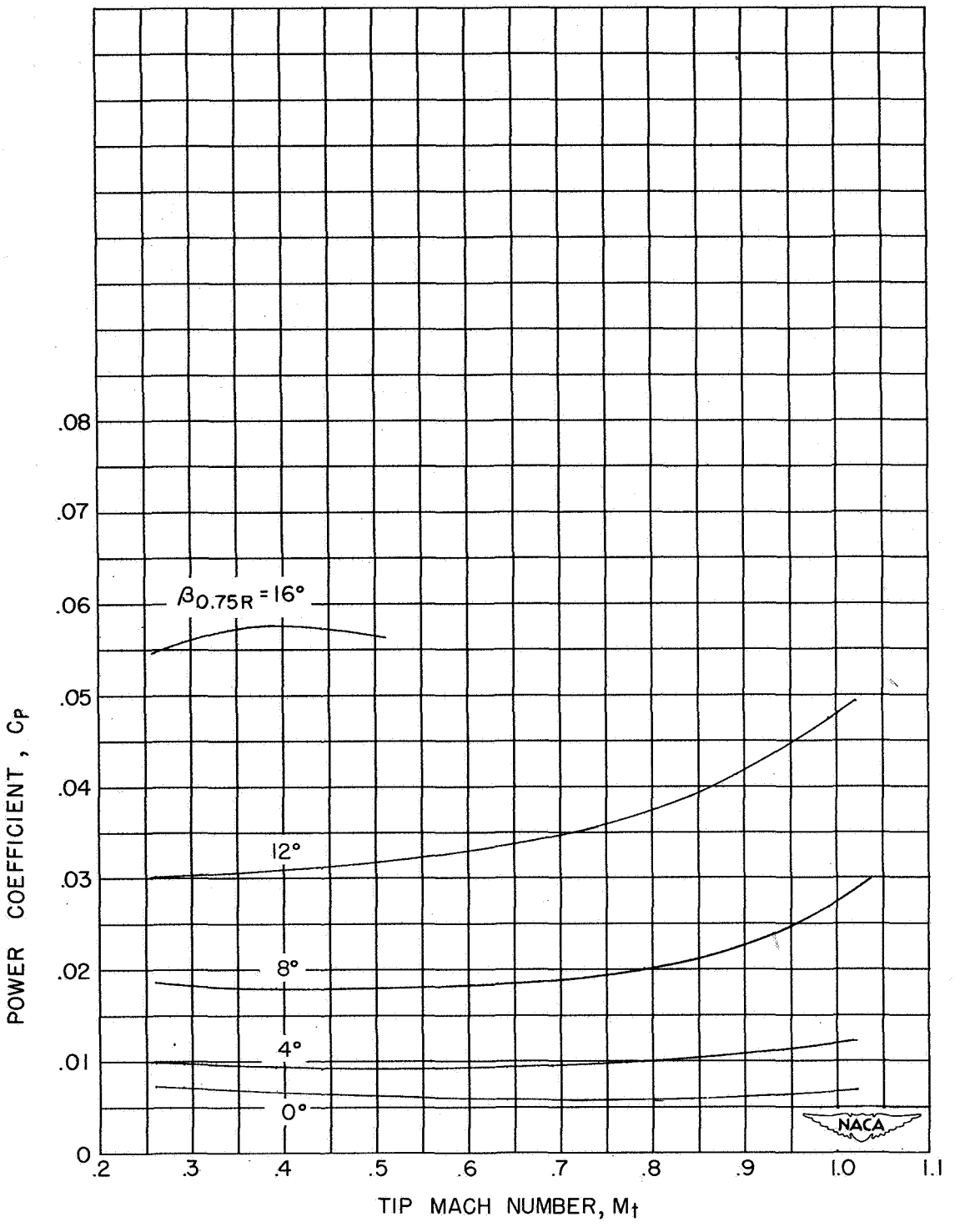

(b) Power coefficient C_P.

Figure 6.- Concluded.

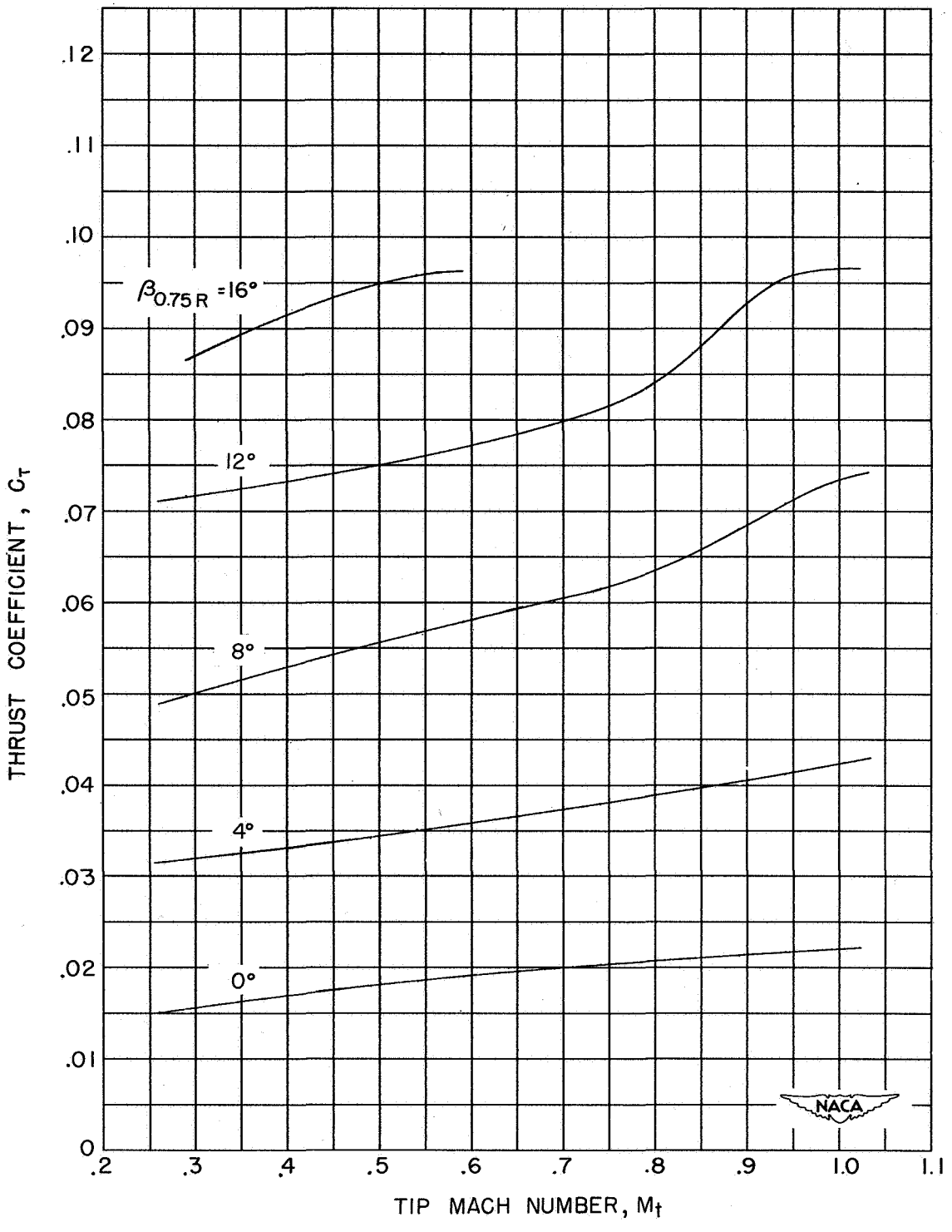

(a) Thrust coefficient C_T.

Figure 7.- Variation of static characteristics with tip Mach number for a two-blade NACA 10-(3)(066)-03 propeller.

[redacted]

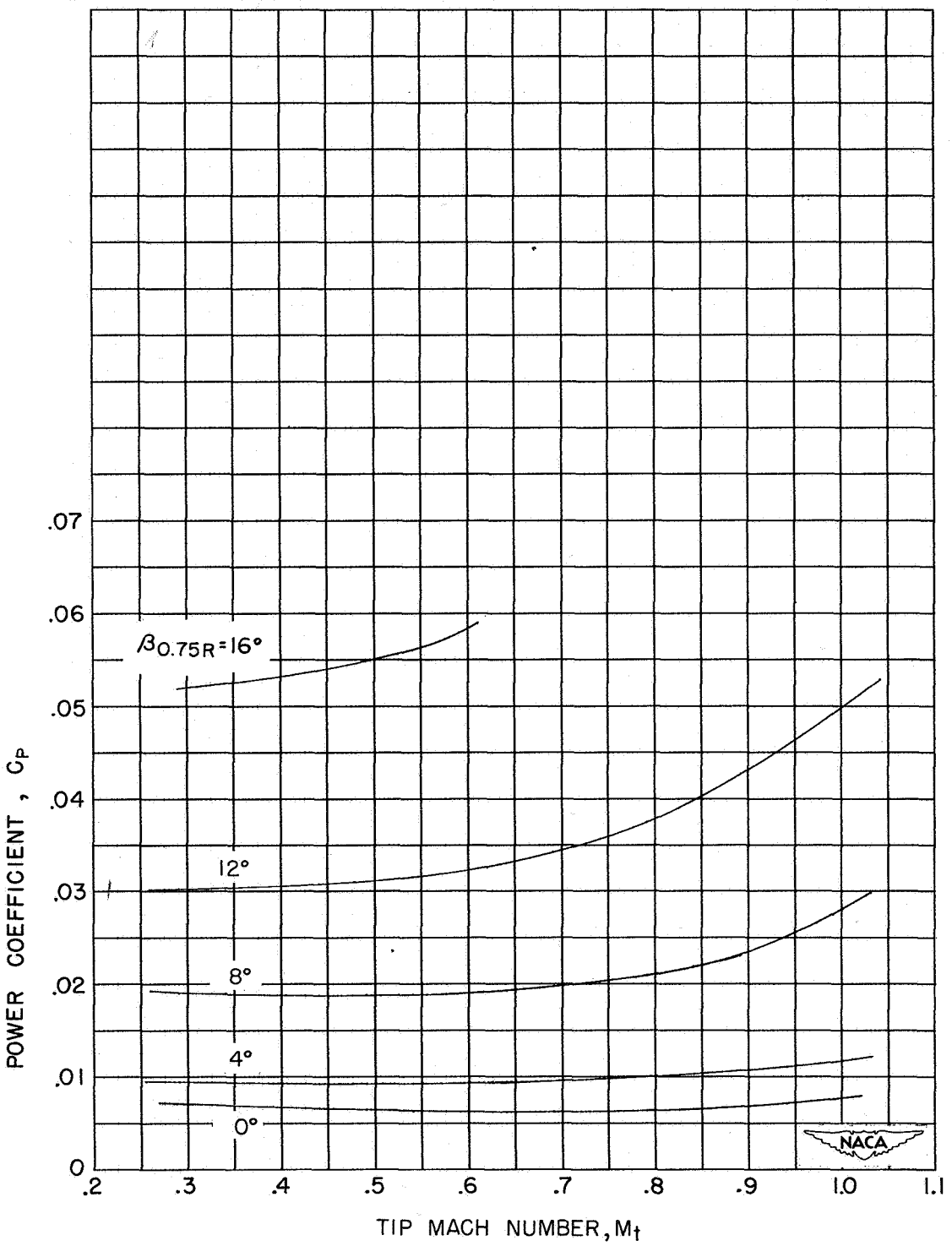

(b) Power coefficient C_P.

Figure 7.- Concluded.

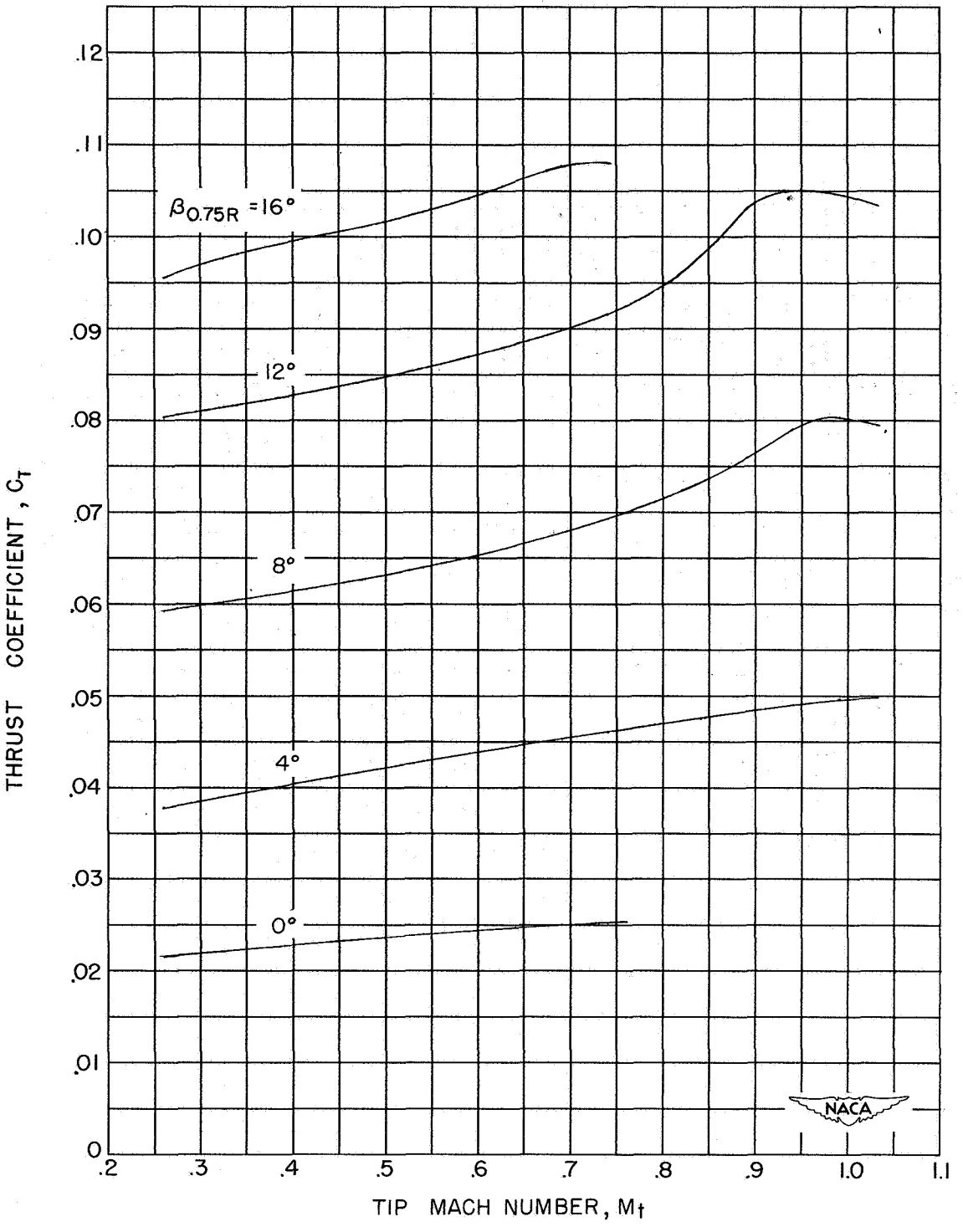

(a) Thrust coefficient C_T.

Figure 8.- Variation of static characteristics with tip Mach number for a two-blade NACA 10-(5)(066)-03 propeller.

[redacted]

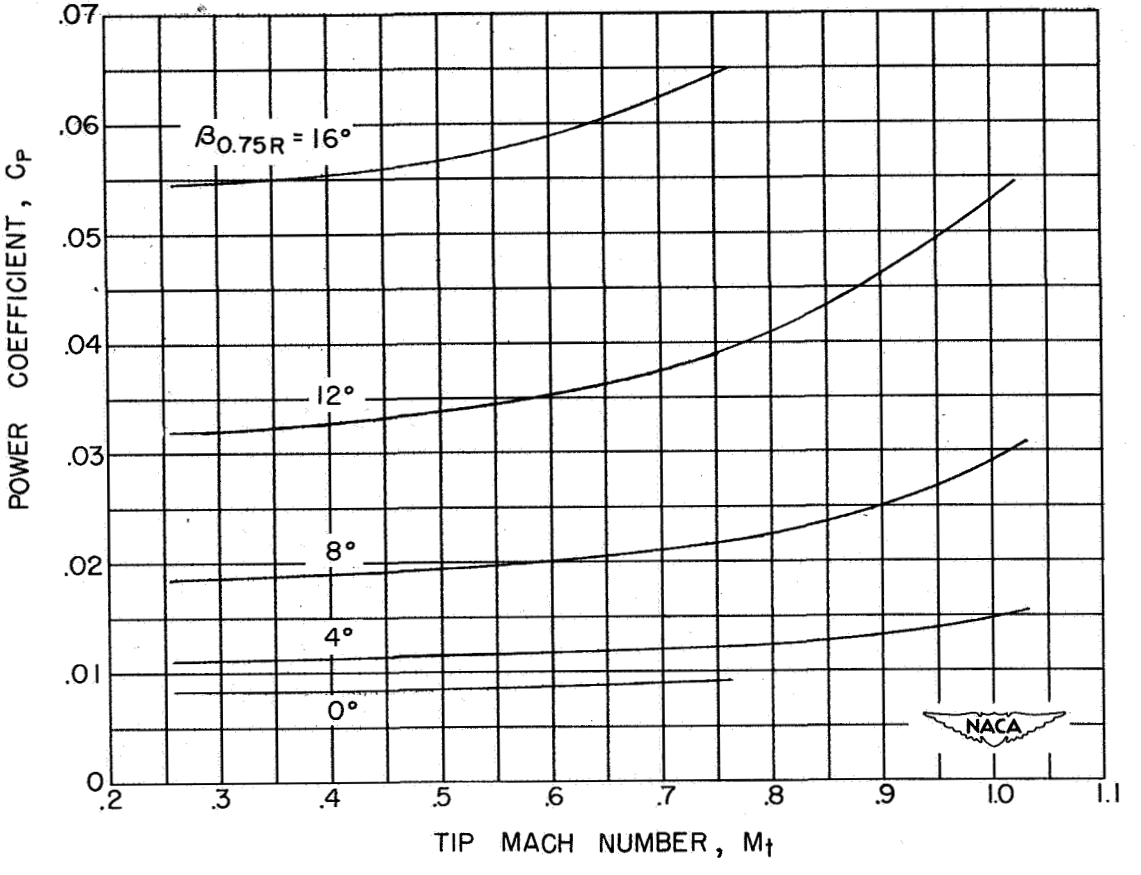

(b) Power coefficient C_P.

Figure 8.- Concluded.

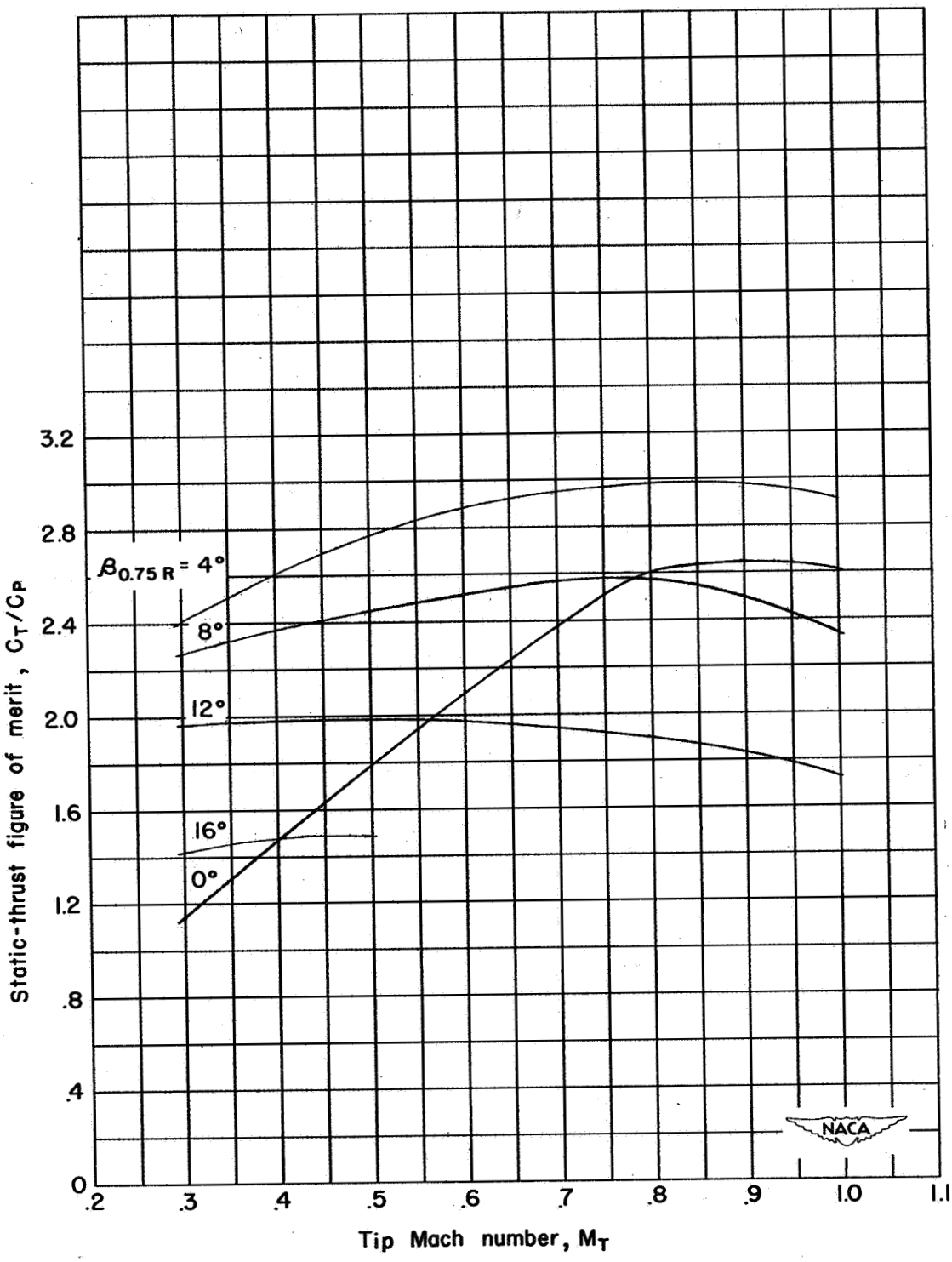

Figure 9.- Variation of static-thrust figure of merit with tip Mach number. NACA 10-(0)(066)-03 propeller.

[redacted]

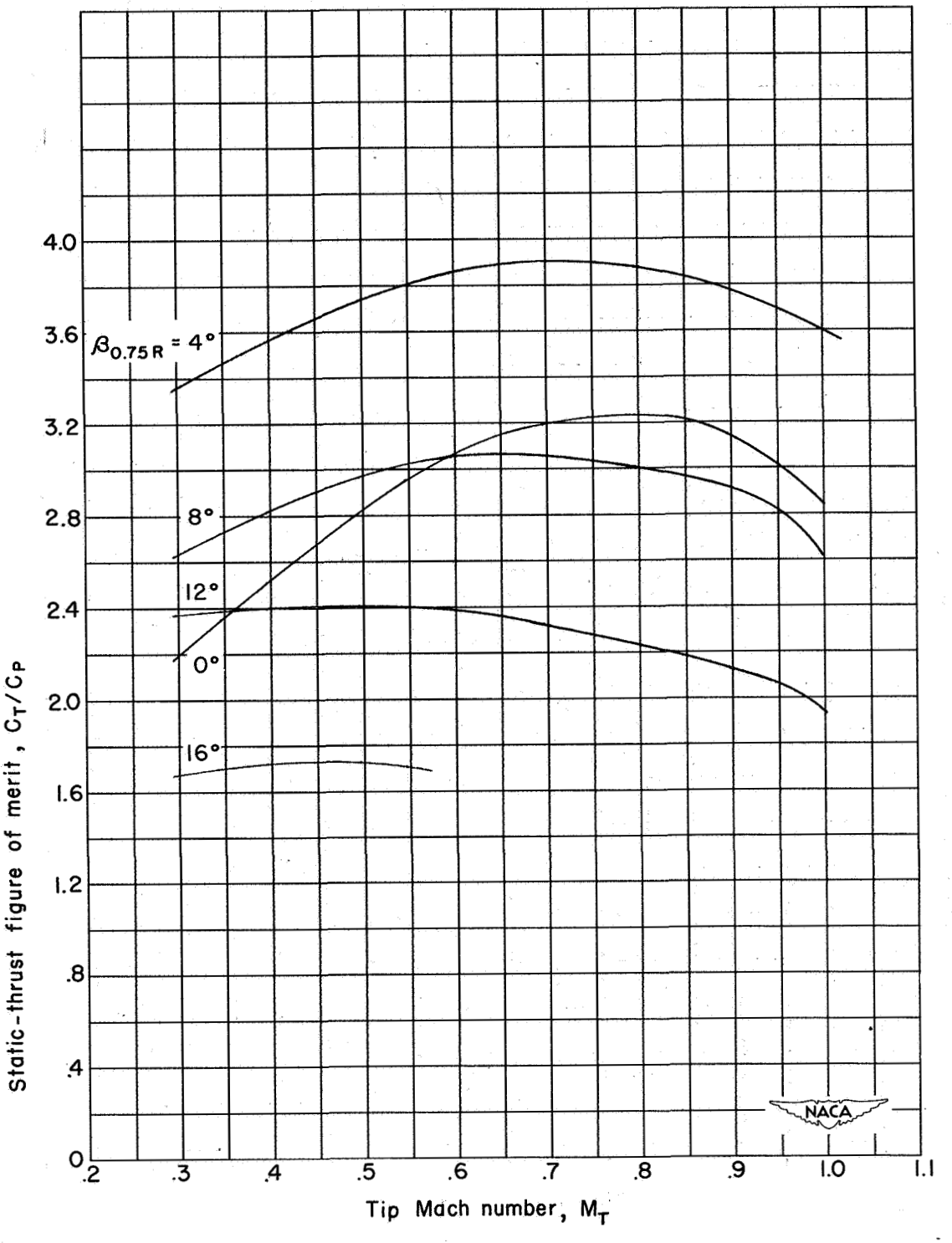

Figure 10.- Variation of static-thrust figure of merit with tip Mach number. NACA 10-(3)(066)-03 propeller.

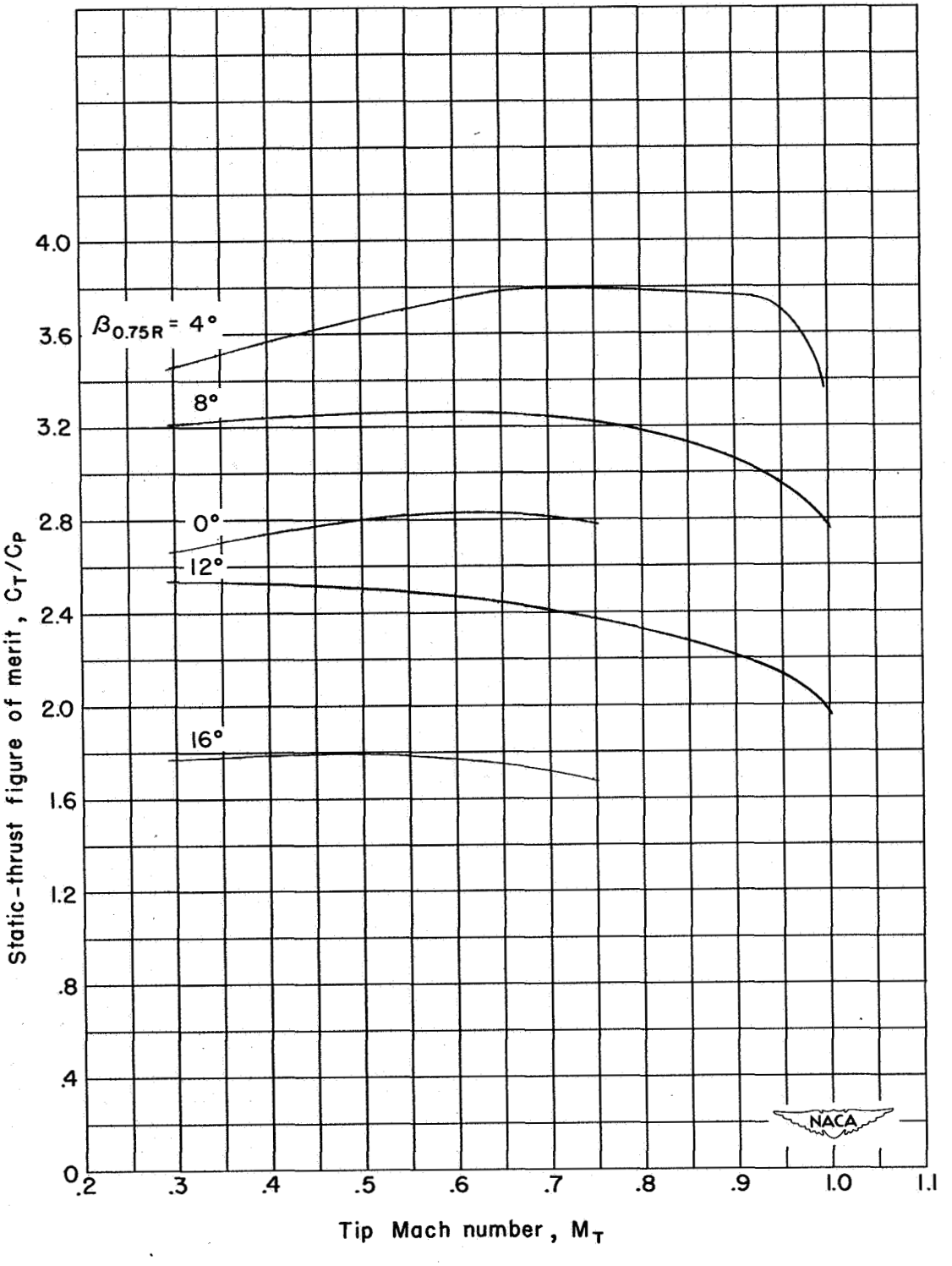

Figure 11.- Variation of static-thrust figure of merit with tip Mach number. NACA 10-(5)(066)-03 propeller.

[redacted]

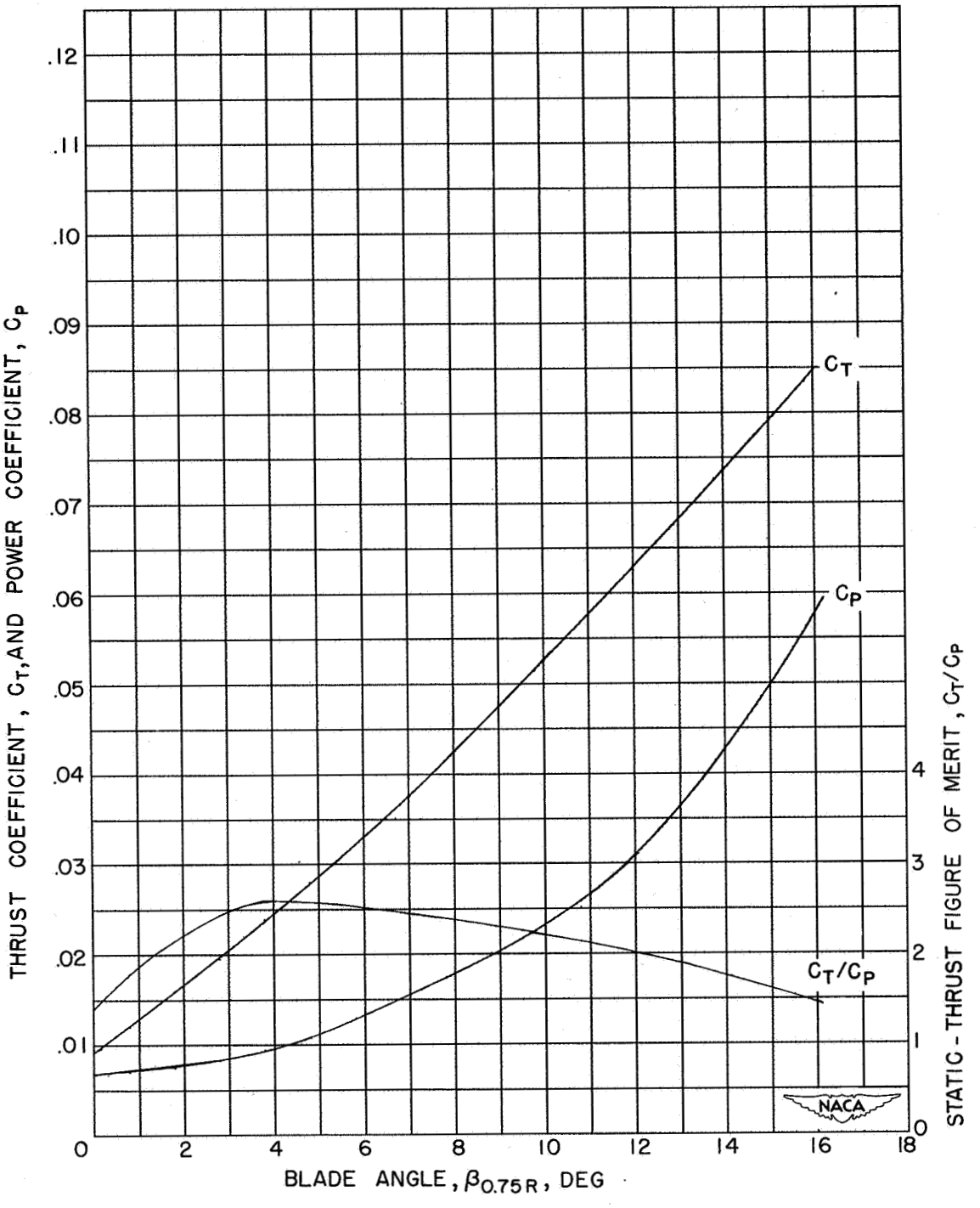

(a) $M_t = 0.4$.

Figure 12.- Variation of static characteristics with blade angle for a two-blade NACA 10-(0)(066)-03 propeller.

[redacted]

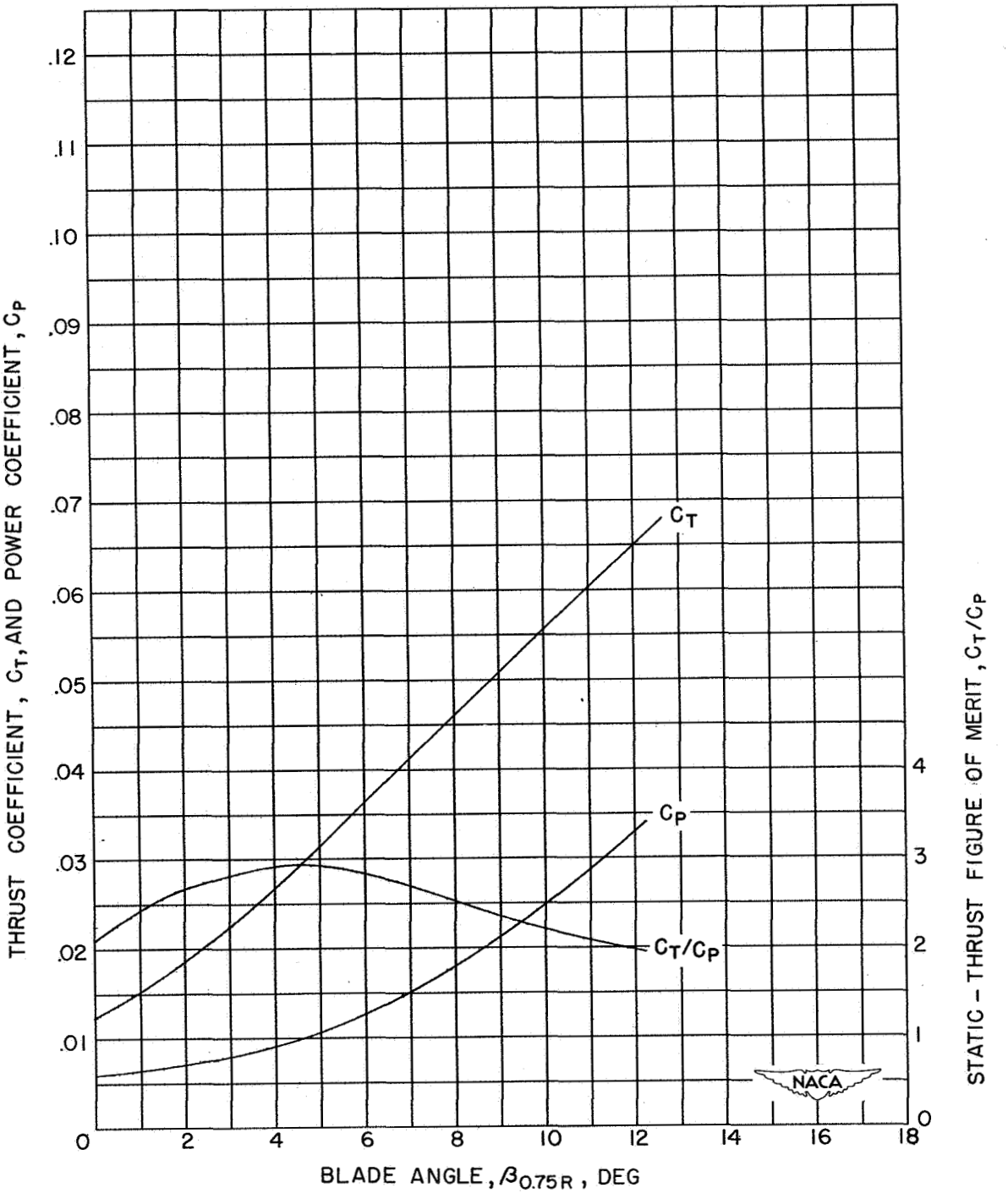

(b) $M_t = 0.6$.

Figure 12.- Continued.

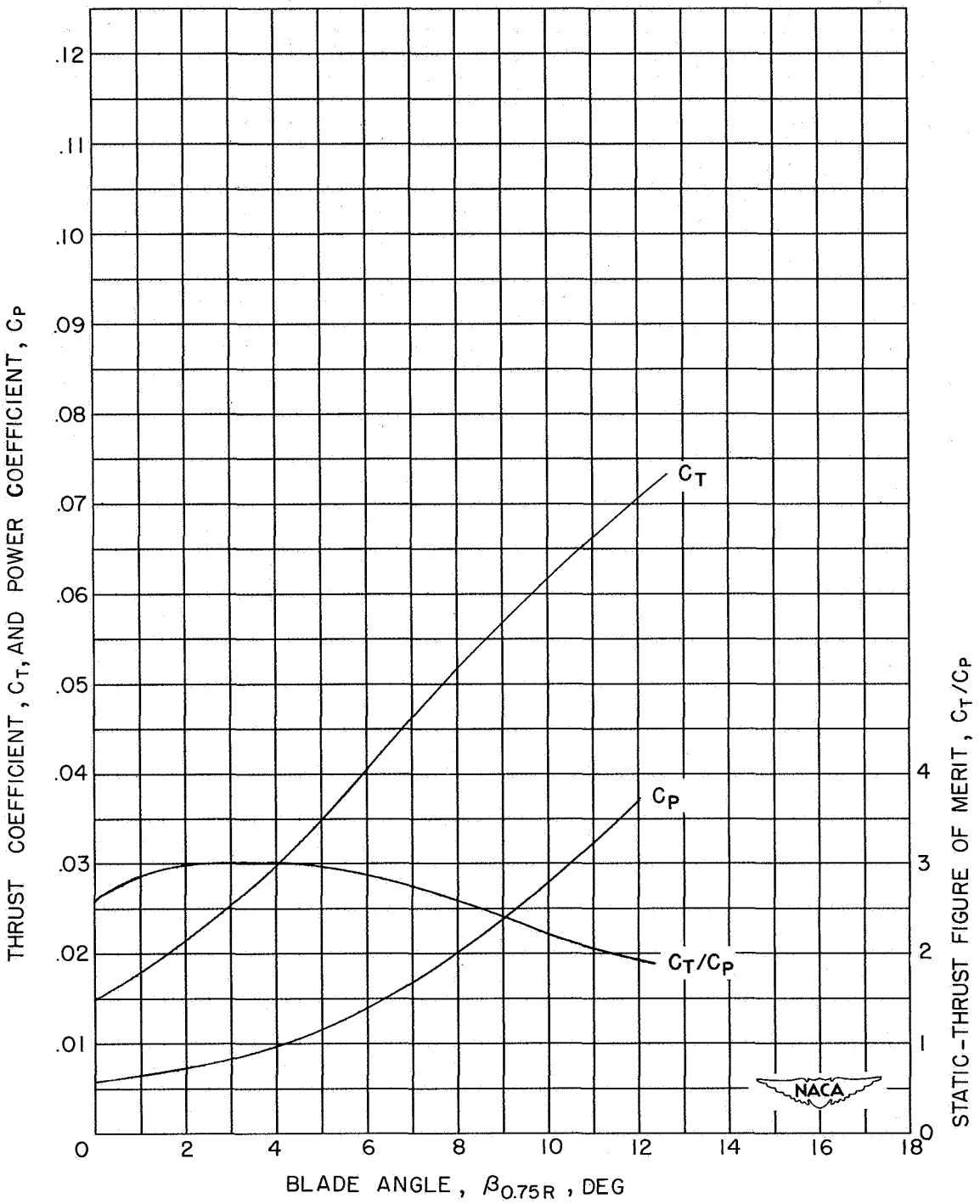

(c) $M_t = 0.8$.

Figure 12.- Continued.

[redacted]

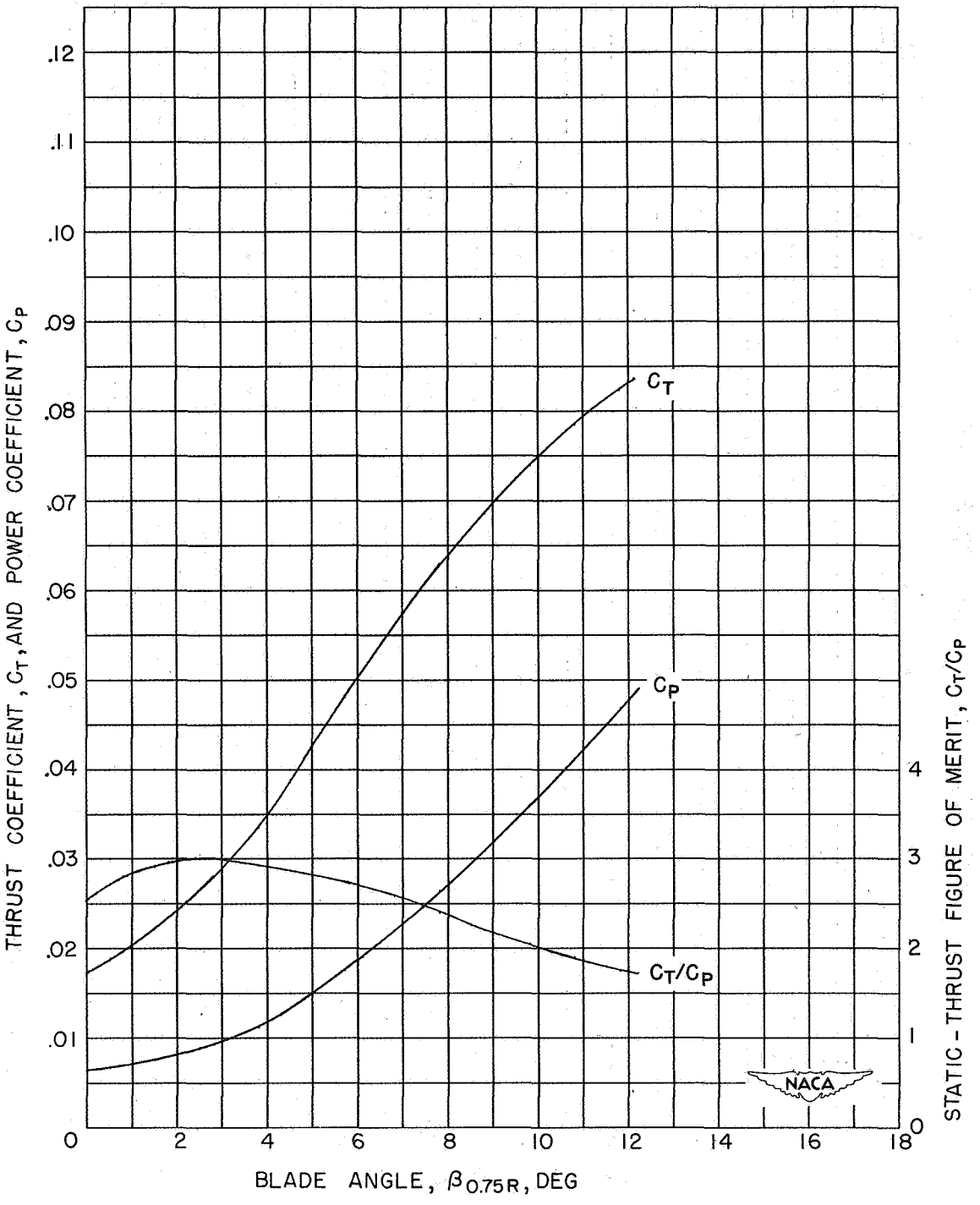

(d) $M_t = 1.0$.

Figure 12.- Concluded.

[redacted]

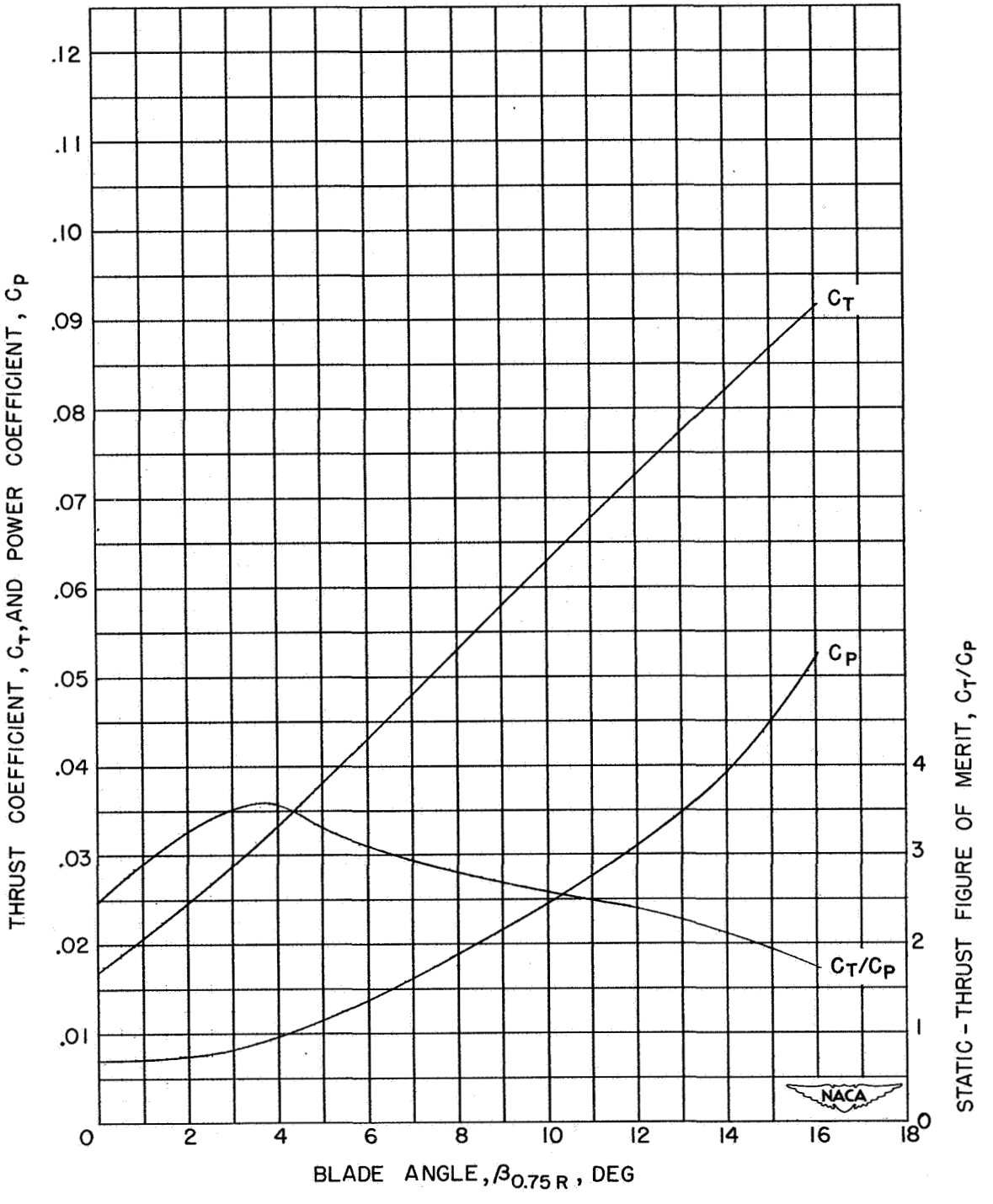

(a) $M_t = 0.4$.

Figure 13.- Variation of static characteristics with blade angle for a two-blade NACA 10-(3)(066)-03 propeller.

[redacted]

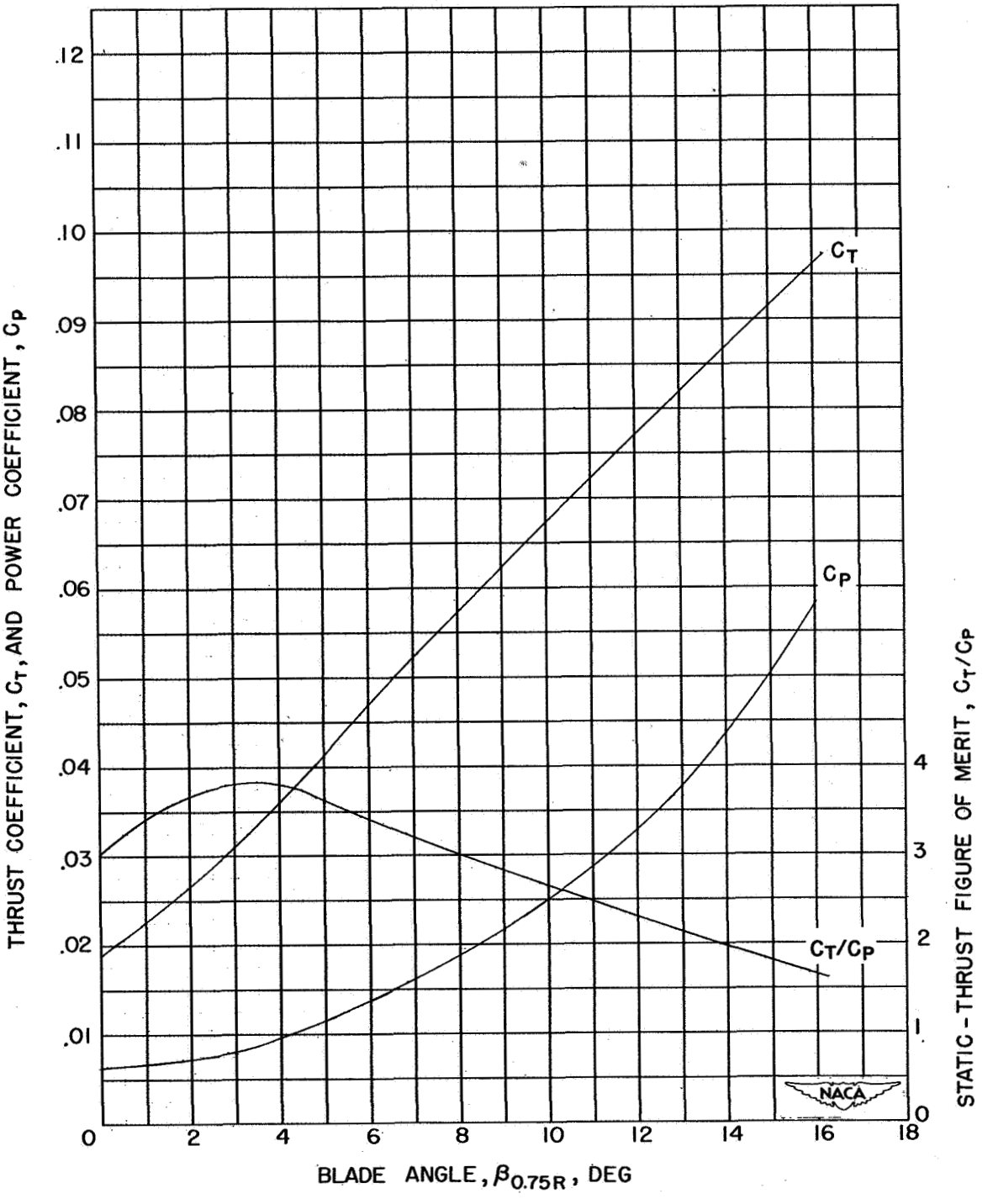

(b) $M_t = 0.6$.

Figure 13.- Continued.

[redacted]

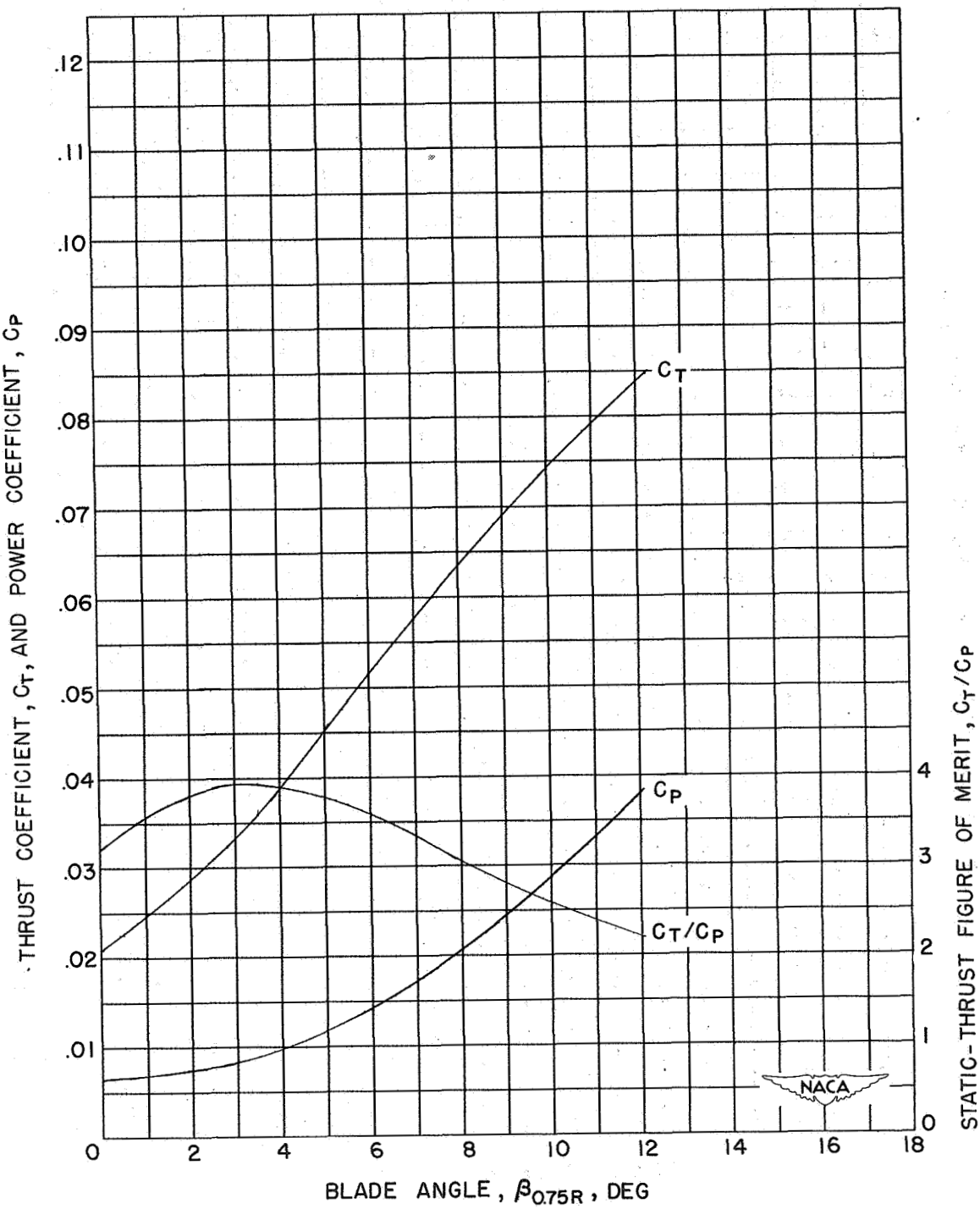

(c) $M_t = 0.8$.

Figure 13.- Continued.

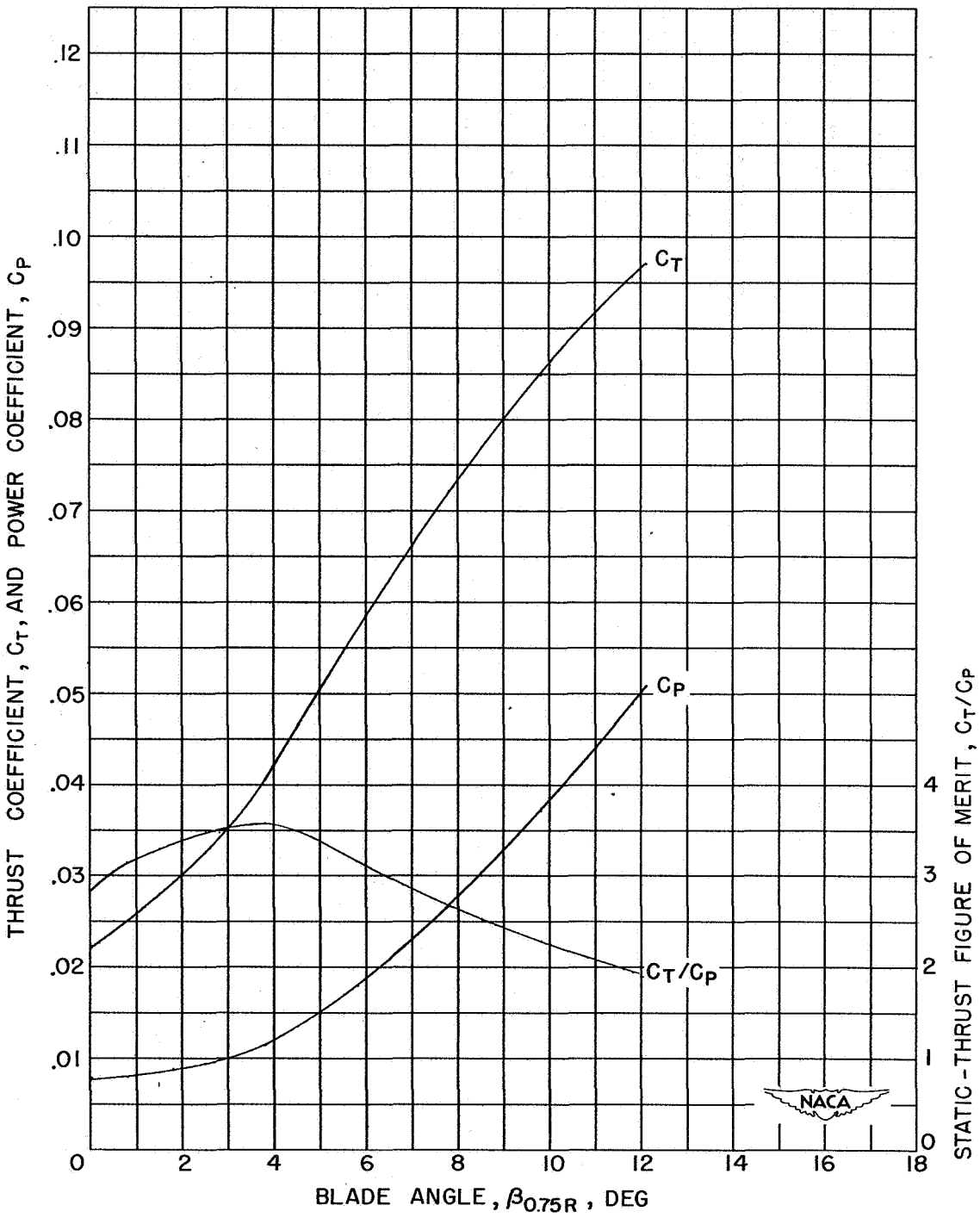

(d) $M_t = 1.0$.

Figure 13.- Concluded.

[redacted]

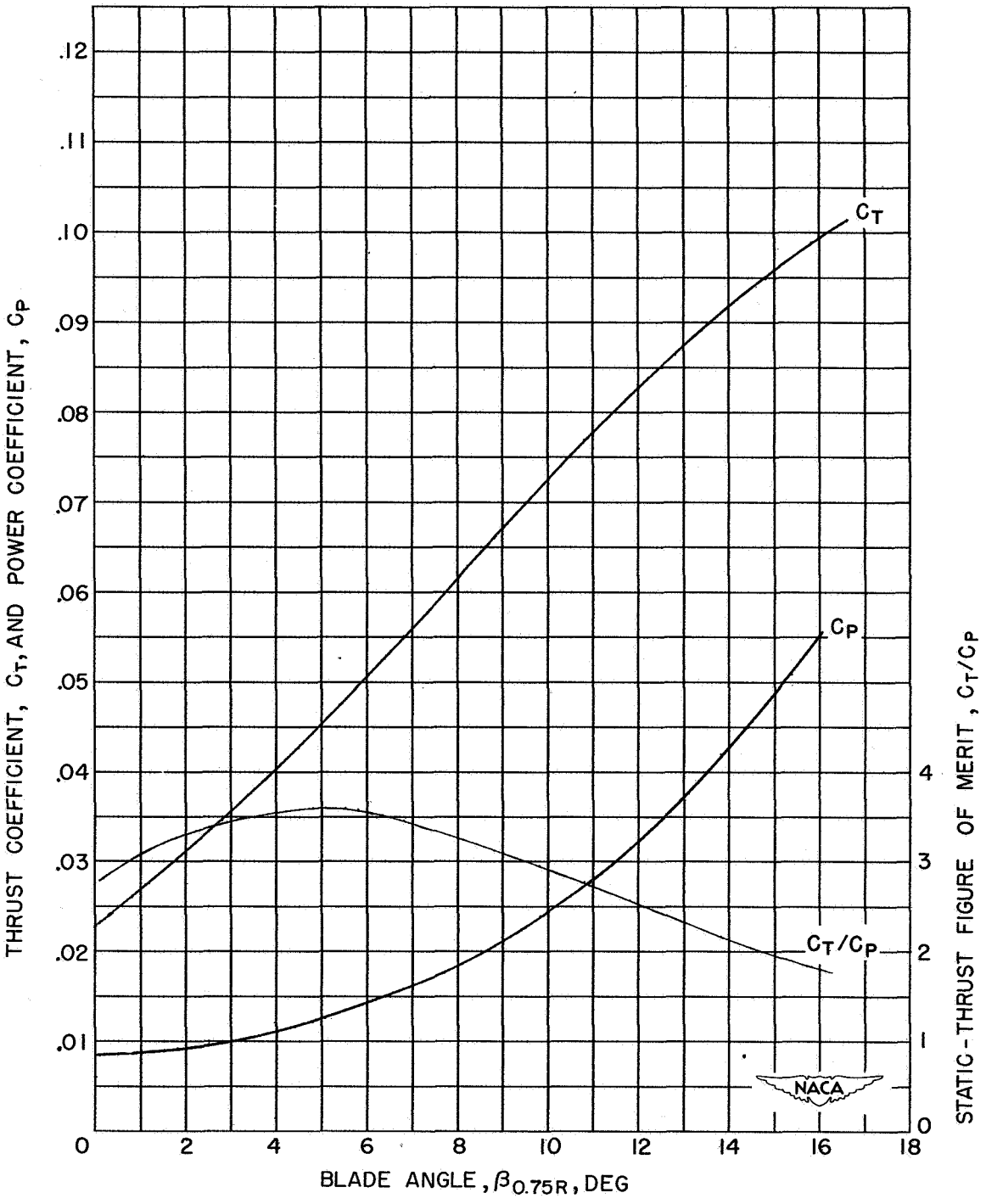

(a) $M_t = 0.4$.

Figure 14.- Variation of static characteristics with blade angle for a two-blade NACA 10-(5)(066)-03 propeller.

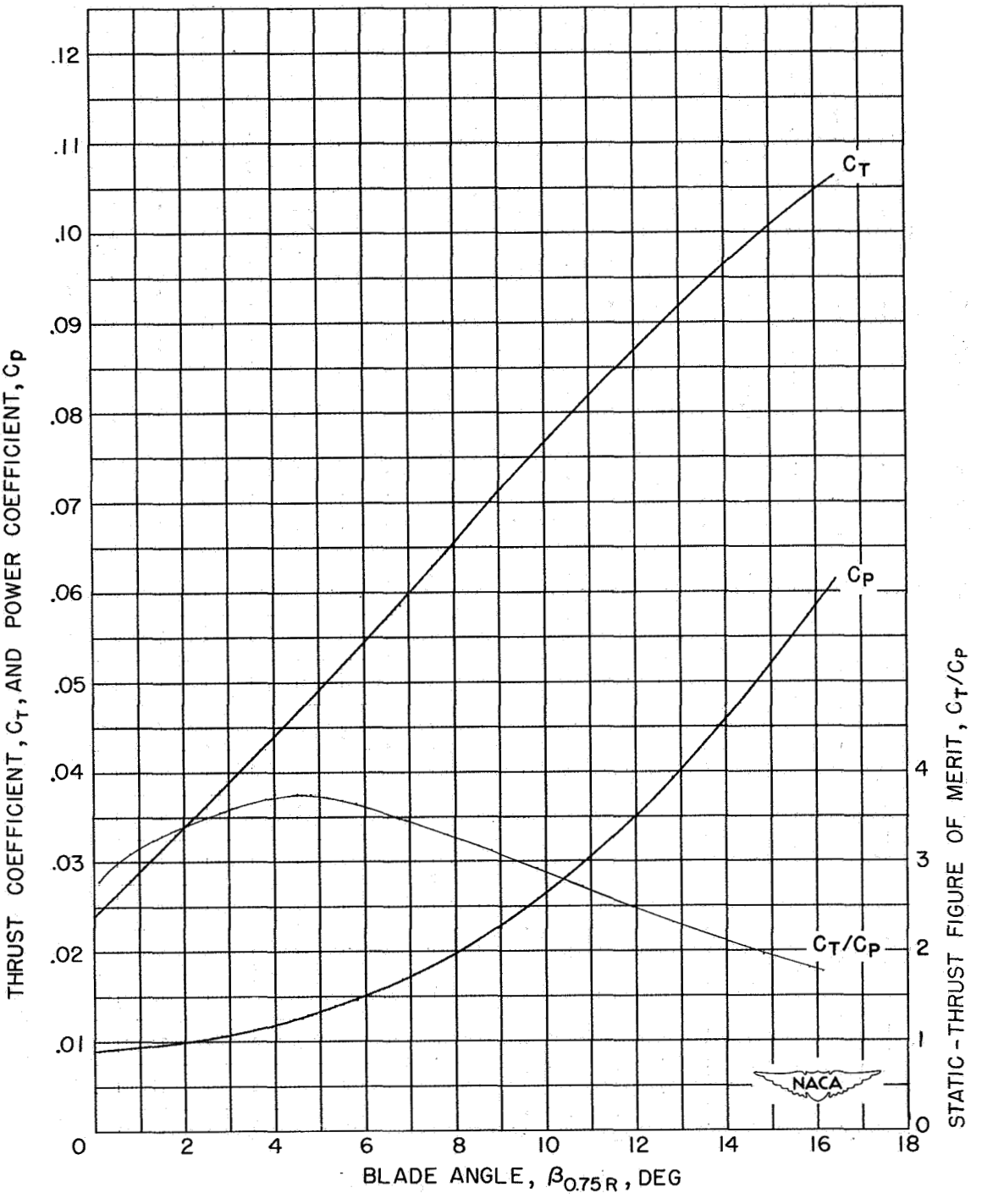

(b) $M_t = 0.6$.

Figure 14.- Continued.

[redacted]

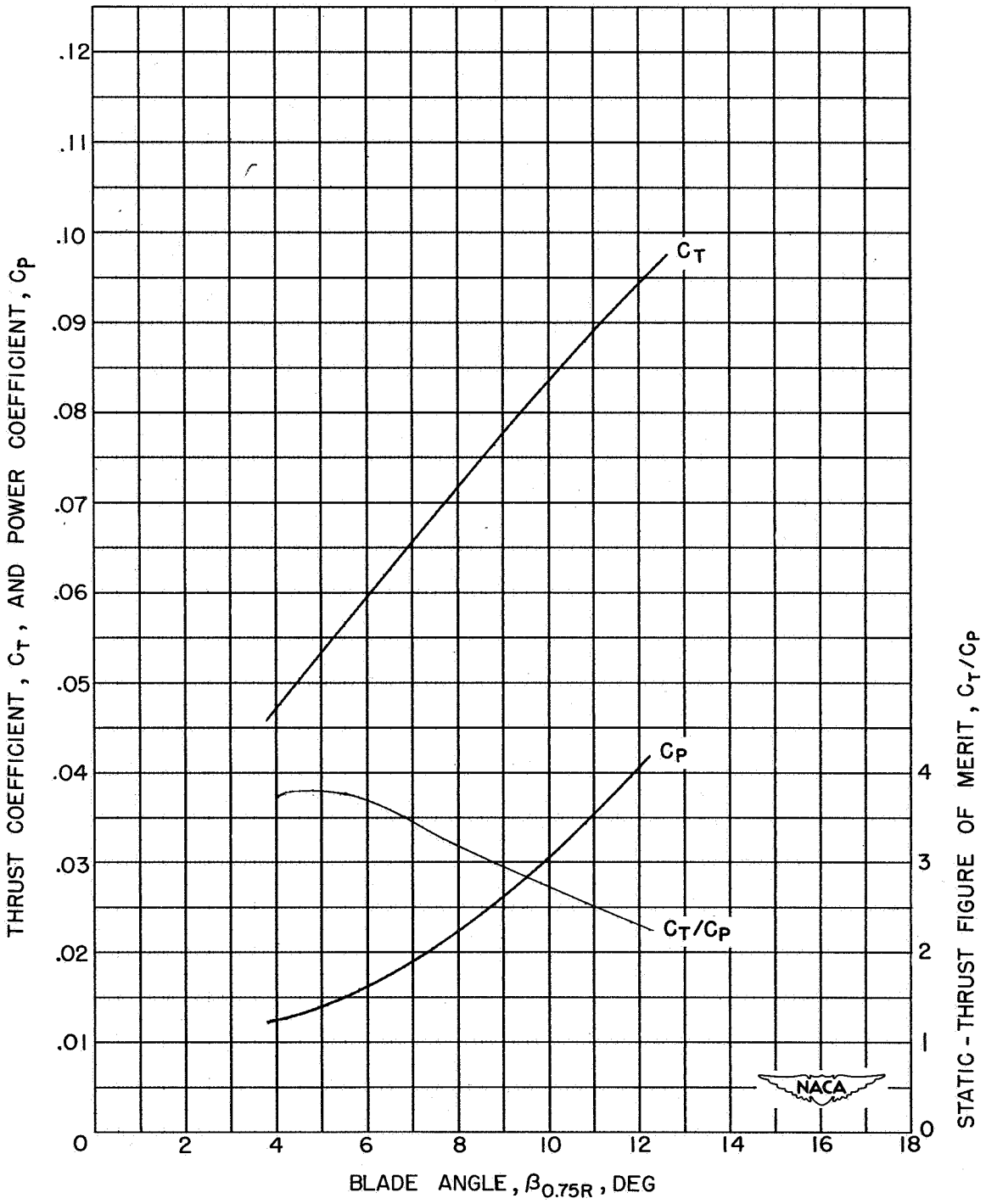

(c) $M_t = 0.8$.

Figure 14.- Continued.

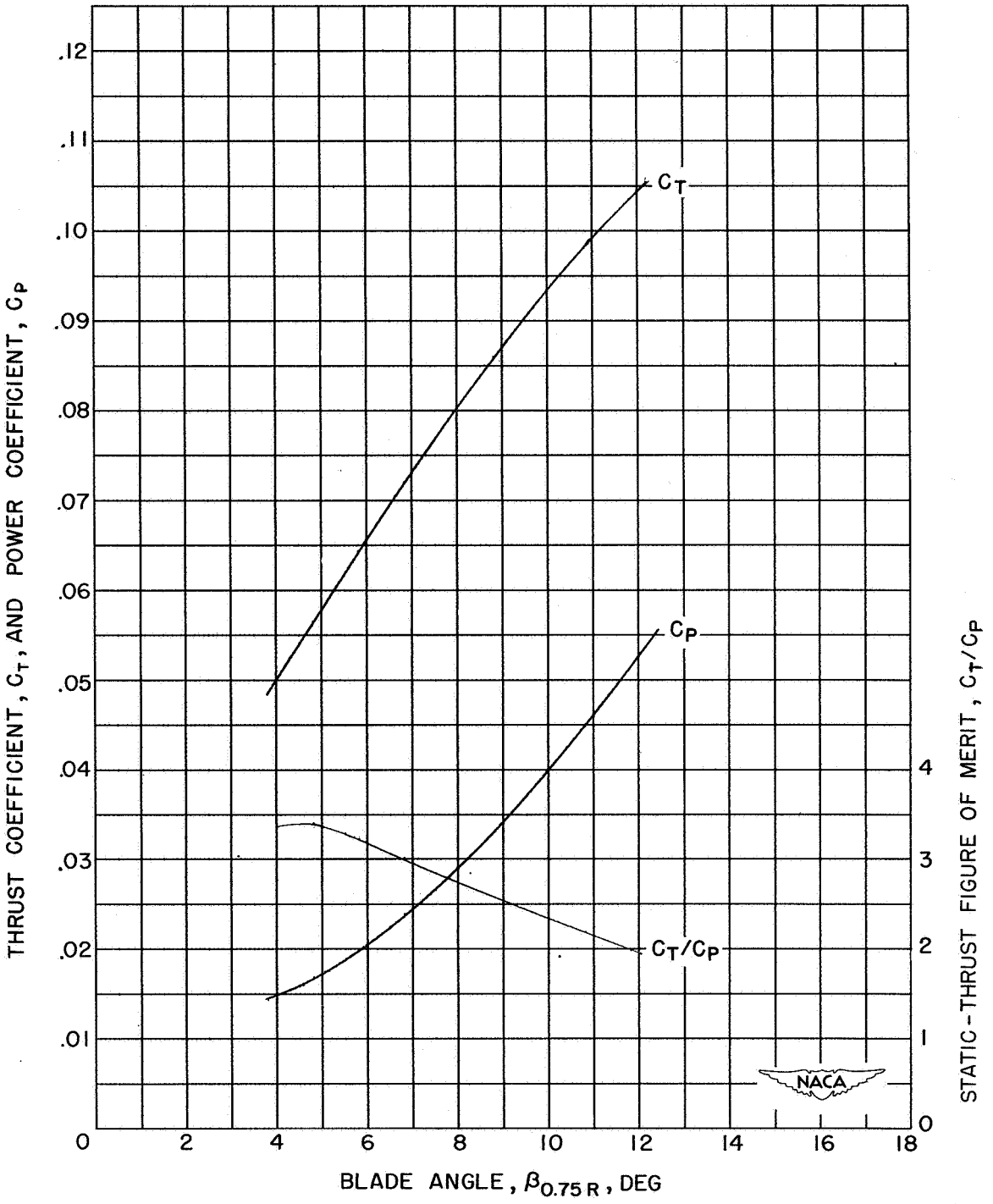

(d) $M_t = 1.0$.

Figure 14.- Concluded.

[redacted]

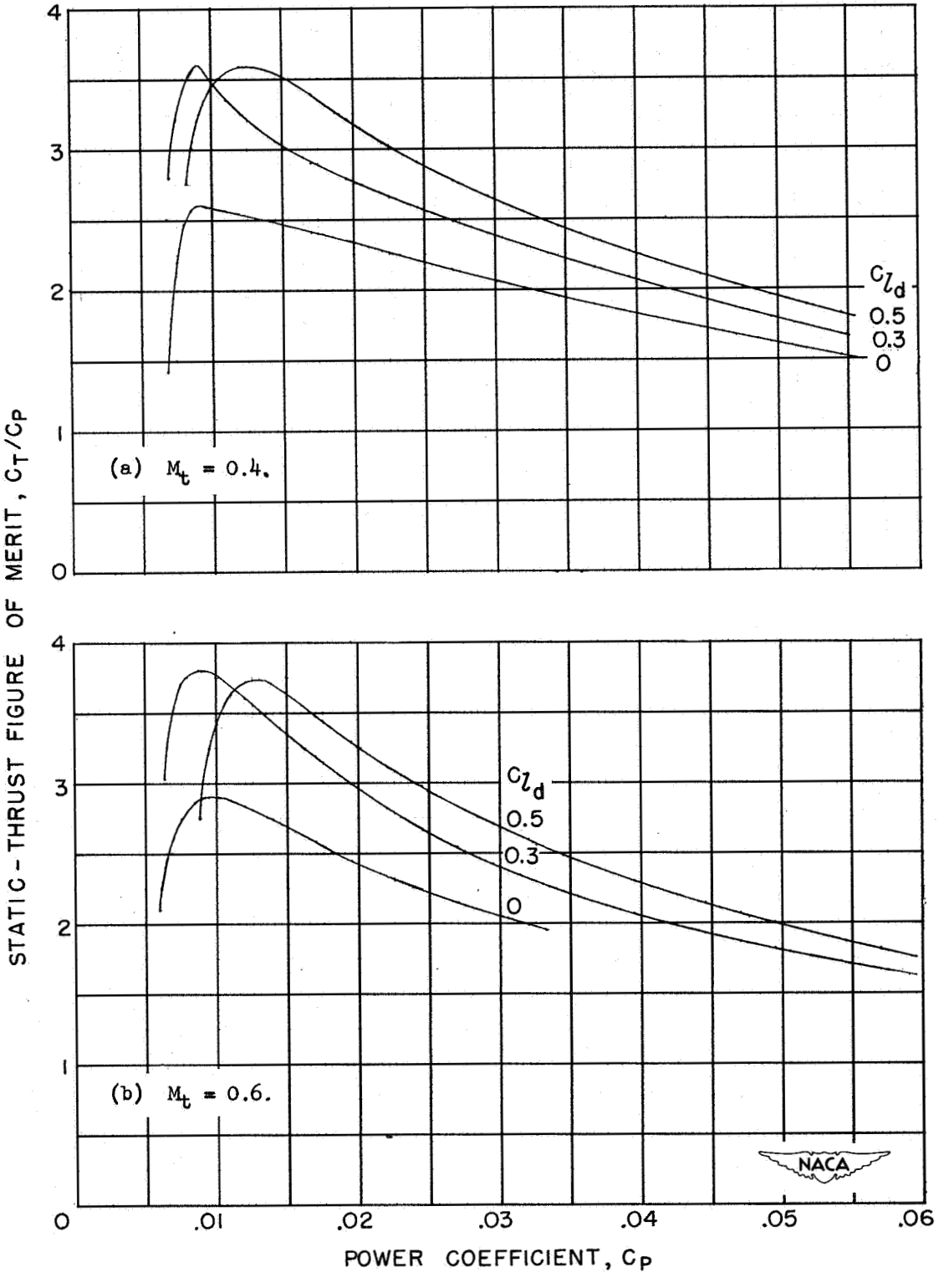

Figure 15.- Variation of static-thrust figure of merit with power coefficient for three NACA propellers.

[redacted]

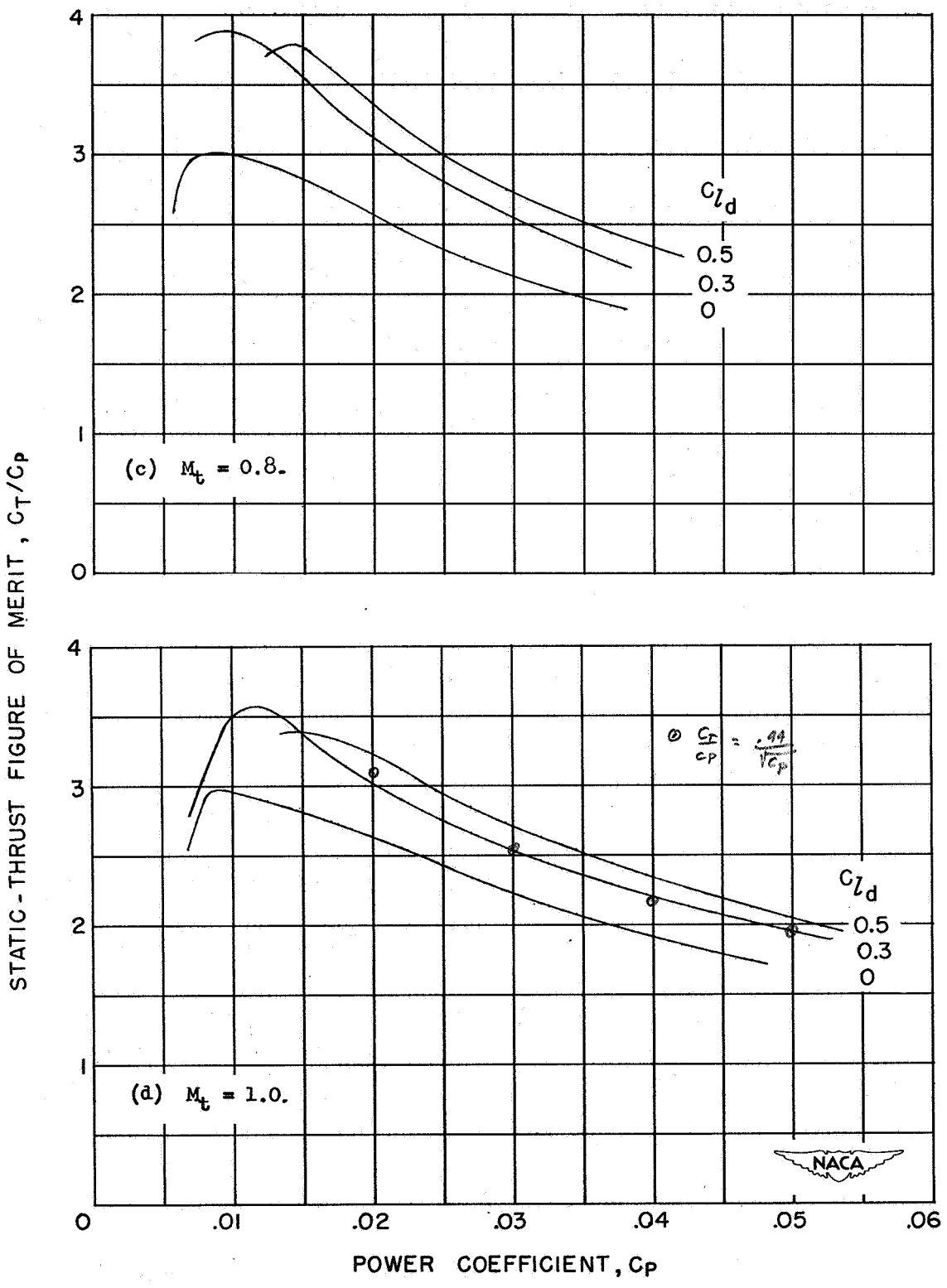

Figure 15.- Concluded.

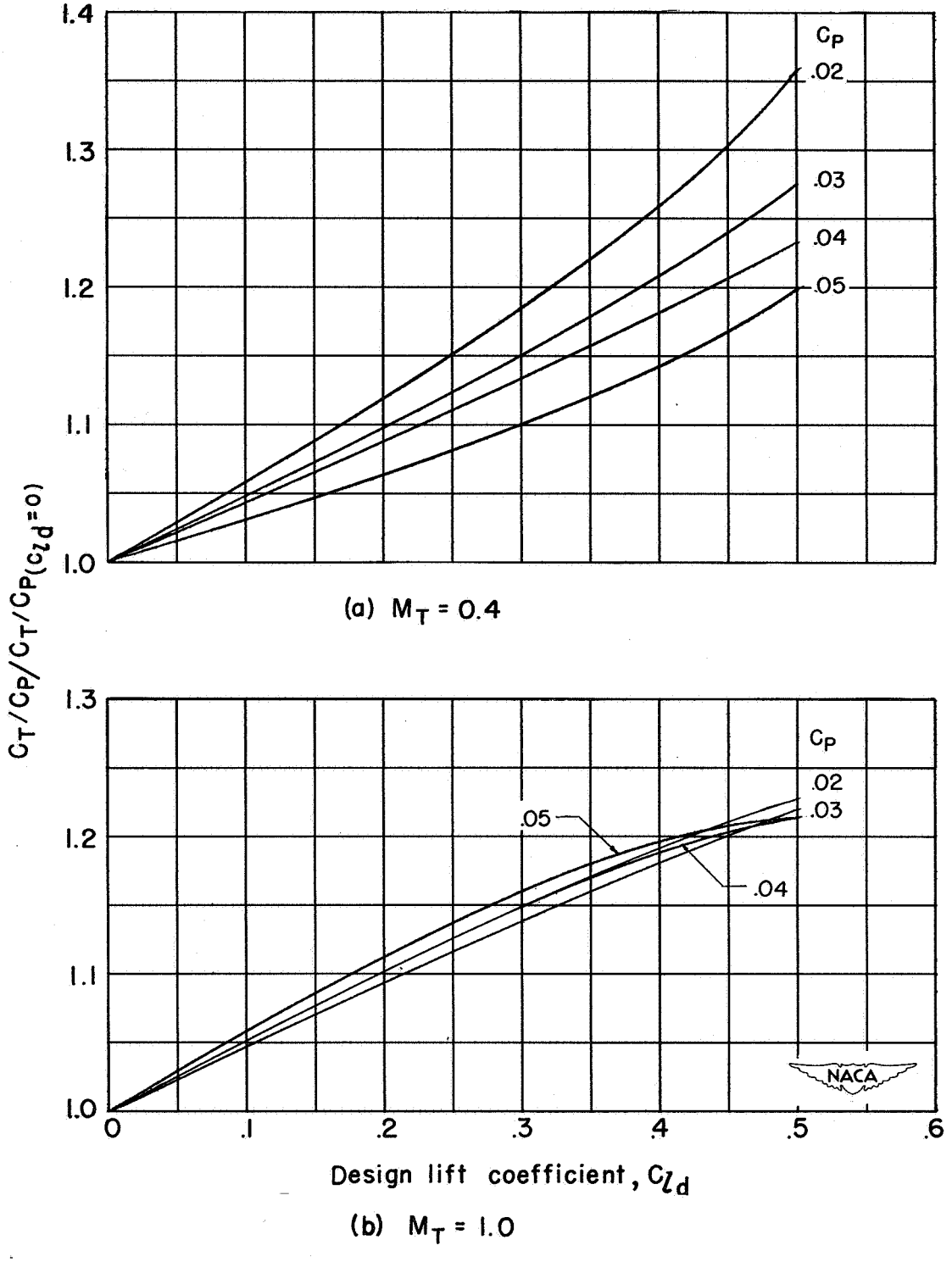

Figure 16.- Increase in ratio $C_T/C_P/C_{T/C_P(C_{l_d}=0)}$ with design lift coefficient for several values of C_P.

[redacted]

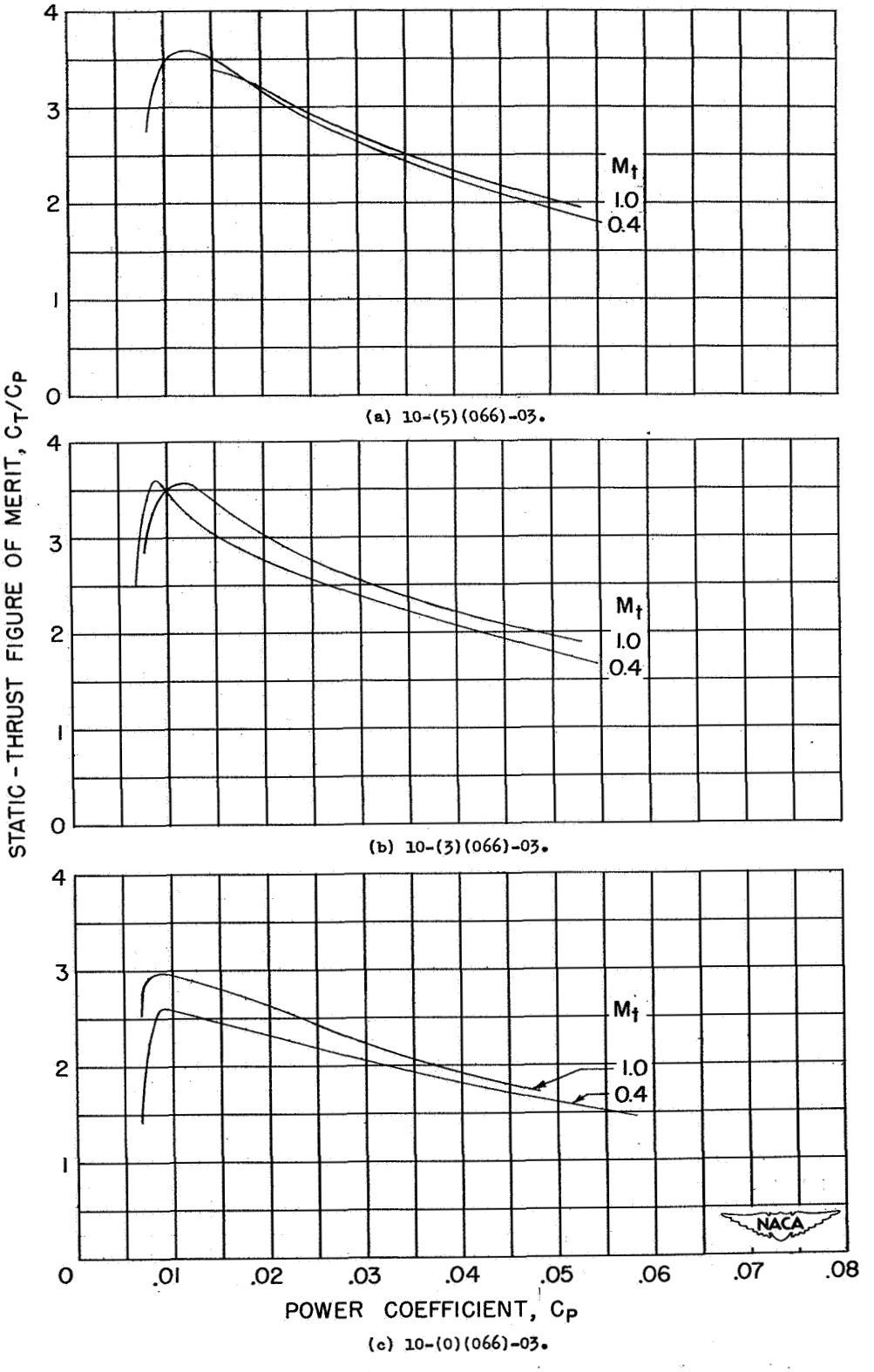

Figure 17.- Effect of tip speed on static-thrust figure of merit for two-blade NACA propellers.

[redacted]

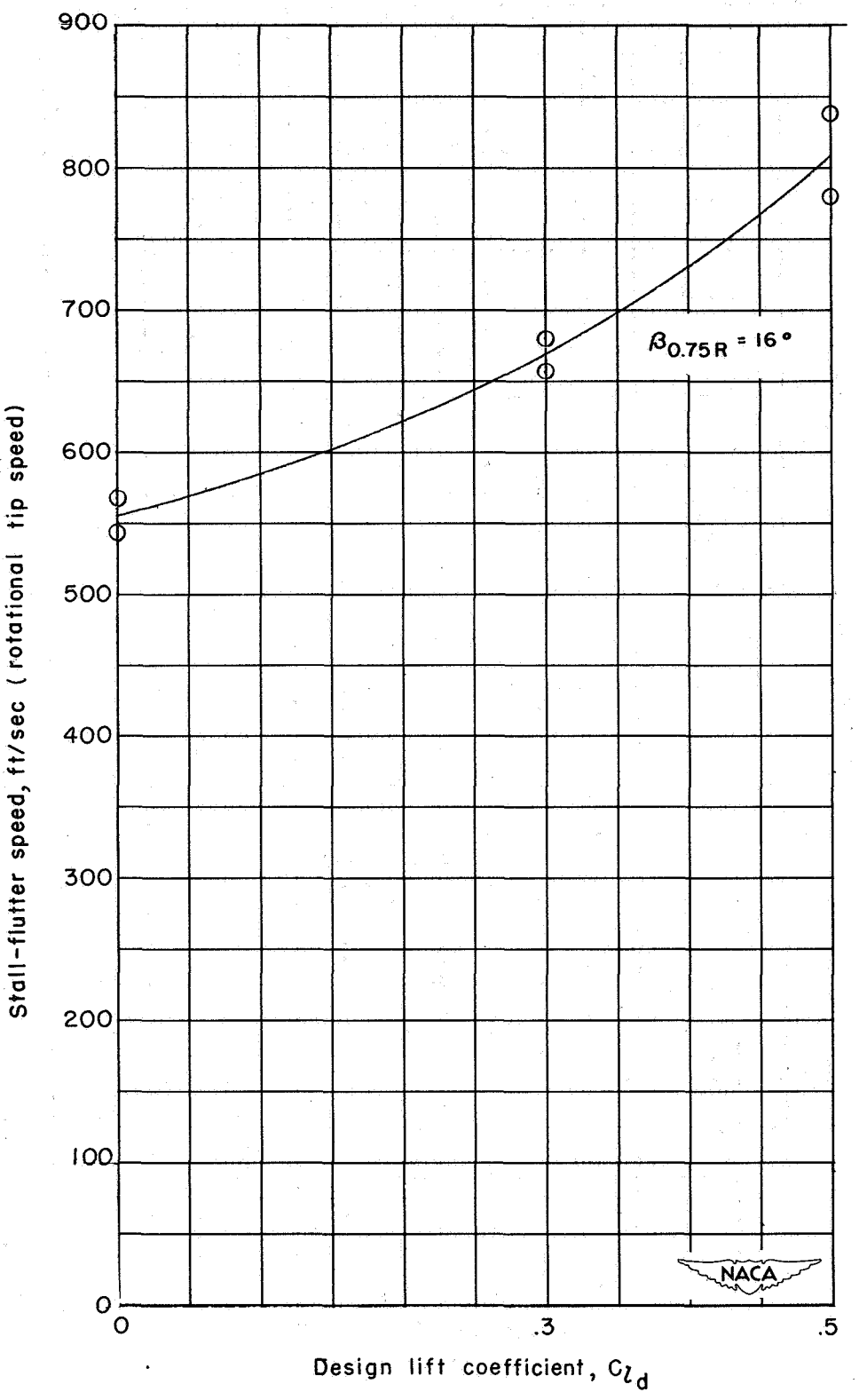

Figure 18.- Variation of stall-flutter speed with design lift coefficient.

[redacted]